ELSEVIER

Contents lists available at ScienceDirect

Brain Research Bulletin

journal homepage: www.elsevier.com/locate/brainresbull



Research report



A holistic rat model to investigate therapeutic interventions in Parkinson's disease: viral induction of a slow-progressing motor phenotype, dopaminergic degeneration and early microglia neuroinflammation

Ekaterini Kefalakes ^{a,b,*,1}, Franziska J. Mewes ^{a,1}, Diana Peristich ^a, Clara Plötner ^a, Volodymyr Shcherbatyy ^{a,†}, Julia Schipke ^c, Friederike Schneider ^a, Christopher Käufer ^d, Regina Rumpel ^e

- ^a Hannover Medical School, Institute of Neuroanatomy and Cell Biology, Carl-Neuberg-Str. 1, Hannover 30625, Germany
- ^b Martin Luther University Halle Wittenberg, Institute of Anatomy and Cell Biology, Groβe Steinstrasse 52, Halle (Saale) 06108, Germany
- ^c Hannover Medical School, Institute for Functional and Applied Anatomy, Carl-Neuberg-Str. 1, Hannover 30625, Germany
- d University of Veterinary Medicine Hannover, Institute of Pharmacology, Toxicology and Pharmacy, Bünteweg 17, Hannover 30559, Germany
- e Hannover Medical School, Institute for Laboratory Animal Science and Central Animal Facility, Carl-Neuberg-Str. 1, Hannover 30625, Germany

ARTICLE INFO

ABSTRACT

Keywords: Parkinson's disease Human α-synuclein Dopaminergic neuron AAV/DJ Motor impairment Parkinson's disease is a chronic progressive neurodegenerative disorder, mostly manifesting in late adulthood. Patients suffering from this idiopathic disease of the nervous system develop cardinal motor symptoms that usually appear after non-motor symptoms. It is characterized by loss of dopaminergic neurons located in the substantia nigra pars compacta and formation of insoluble intracellular protein inclusions of α-synuclein (Lewy Bodies). Another symptom is neuroinflammation, which often precedes dopaminergic neuron degeneration and the formation of aggregates. In this study, we aimed to establish a viral vector-mediated rat model of Parkinson's disease that mimics both the histological features of the disease and its slow, age-related progression, including the development of a motor phenotype over time. Evaluation of different adeno-associated viral serotypes overexpressing the human α-synuclein protein revealed that both AAV/6 and AAV/DJ equally transduce primary dopaminergic neurons in vitro with the latter being more efficient. In vivo transduction of dopaminergic neurons with AAV/DJ led to their degeneration in the substantia nigra pars compacta, which coincided with reduced dopaminergic fibers reaching the ipsilateral striatum. Microglia inflammatory response and accumulation thereof was evident at early disease stages. Simultaneously, behavioral assessment in the cylinder, the stepping and the staircase test showed a decrease in gross motor performance while rearing and stepping. Taken together, we established an early AAV/DJ-mediated model for Parkinson's disease in rats, which not only shows histological hallmarks but due to its progressive motor phenotype also provides a therapeutic window suitable for future pharmacological modification.

1. Introduction

Parkinson's disease (PD) is a chronic, progressive neurodegenerative disease affecting the elderly, as 1 in 100 people over 60 is prone to develop PD (de Rijk et al., 2000; Rajput, 1992). Furthermore, the risk of developing PD is constantly increasing as the world's population is also

aging (Tysnes, Storstein, 2017; Dorsey et al., 2018; Tumas et al., 2025). This renders PD a socioeconomic burden on the health care system, due to emerging costs from hospitalizations, pharmacological treatment, outpatient visits and home care regarding patients and caregivers (Soundy et al., 2014; GBD, 2016; Su et al., 2025).

Patients show a plethora of clinical symptoms, with the cardinal ones

https://doi.org/10.1016/j.brainresbull.2025.111464

^{*} Corresponding author at: Martin Luther University Halle Wittenberg, Institute of Anatomy and Cell Biology, Große Steinstrasse 52, Halle (Saale) 06108, Germany. E-mail addresses: Ekaterini.Kefalakes@medizin.uni-halle.de (E. Kefalakes), fj.mewes@gmx.de (F.J. Mewes), diana.peristich@zmnh.uni-hamburg.de (D. Peristich), Clara.L.Ploetner@stud.mh-hannover.de (C. Plötner), vshcherbatyy@gmail.com (V. Shcherbatyy), schipke.julia@mh-hannover.de (J. Schipke), Fschneider@schneidernetworks.de (F. Schneider), christopher.kaeufer@tiho-hannover.de (C. Käufer), Regina.Rumpel@uni-bielefeld.de (R. Rumpel).

First authors contributed equally

[†] Deceased

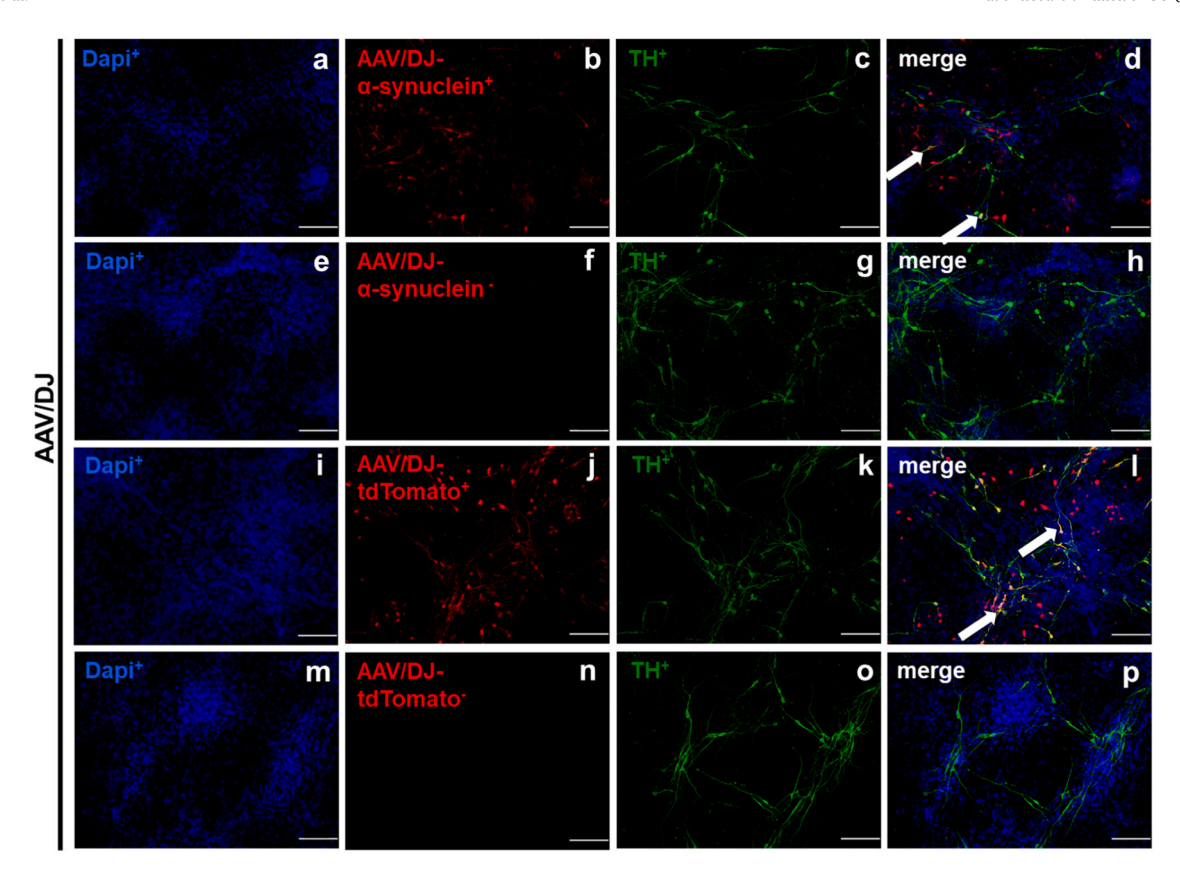


Fig. 1. Transduction potential of the AAV/DJ serotype overexpressing the human α-synuclein protein. Assessment of transduction potential of AAV/DJ-α-synuclein and AAV-DJ/tdTomato in primary DA neurons. 80.000 cells were seeded per well and differentiated for 3 days. After 3 DIV, cells were transduced with 1×10^{10} vg/μL AAV/DJ-α-synuclein or AAV/DJ-tdTomato for 3 days, respectively. After 8 DIV, all cells were fixed and stained for TH (green) and Dapi (blue). AAV/DJ-α-synuclein transduced cells were additionally stained for α-synuclein (red), while fluorescence of tdTomato (red) in AAV/DJ-tdTomato transduced cells was directly visualized without additional staining. Representative immunocytochemical stainings of DA neurons transduced with AAV/DJ-α-synuclein (a-d), AAV/DJ-tdTomato (i-l) and control DA neurons with no viral transduction (AAV/DJ-α-synuclein (e-h) and AAV/DJ-tdTomato (m-p), respectively). White arrows point towards transduced TH⁺ cells (d and l). All images were acquired with a 20 × magnification objective. Scale bar is 100 μm.

affecting initiation and fine regulation of movement, including resting tremor, rigidity, bradykinesia and postural instability (Goetz, 2011). Apart from motor impairment, non-motor symptoms like dementia, depression, anxiety and sleep disorders also occur (Takamatsu et al., 2018). The progression of motor symptoms coincides with the depletion of the neurotransmitter dopamine in the *striatum* (STR), which is the result of a loss of dopaminergic (DA) neurons located in the *substantia nigra pars compacta* (SNpc) (Ehringer et al., 1961; Fearnley and Lees, 1991). Degeneration of the SNpc leads to the dysregulation of the basal ganglia circuitry of the nigostriatal system, which plays a critical role in the coordination of controlled movement (Barbeau et al., 1961; Lloyd and Hornykiewicz, 1970). Clinical signs of PD patients become evident when 80 % of striatal DA innervation is lost and 50 % of DA neurons of the SNpc are degenerated (Marsden, 1990).

Loss of DA neurons is linked to the accumulation of proteinaceous aggregates of α -synuclein, which further renders PD a synucleinopathy. Physiologically, α -synuclein is involved in the N-ethylmaleimide-sensitive-factor attachment protein receptor (SNARE)-complex mediated vesicular neurotransmitter release, axonal transport and autophagy (Ben Gedalya et al., 2009; Burré et al., 2010; Maroteaux et al., 1988; Perez et al., 2002). Alpha-synuclein misfolds and aggregates in the form of insoluble intraneuronal inclusions, so called Lewy bodies (LBs) and Lewy neurites (LNs), the pathological hallmarks of PD (Gibb and Lees, 1988; Spillantini et al., 1997). Genome-wide association studies categorize single nucleotide polymorphisms in the gene and promoter region of α -synuclein as a risk factor for PD and analysis of postmortem brain tissue suggests that disease progression is proportional to the spreading of α -synuclein aggregates throughout the brain as LBs can be found in

cortical areas, the amygdala, locus coeruleus, the vagal nucleus and the peripheral autonomic system (Braak et al., 2003; Grover et al., 2022; Wakabayashi and Takahashi, 1997).

Although PD is an idiopathic disease, a genetic heredity is evident in $5{\text -}10\,\%$ of the patients suffering from PD. Monogenetic causes can be traced back to mutations in genes such as SNCA, LRKK2, PINK1, DJ-2 or Parkin (Jia et al., 2022). The most frequent autosomal dominant genetic mutation causing the onset of PD is LRRK2, while mutations of the SNCA gene only appear with a rare frequency of up to 1,1 %. (Hernandez et al., 2016; Jia et al., 2022, Ye et al., 2023). These mutations are encoding for α -synuclein or multiplications of its locus (Polymeropoulos et al., 1997; Wong and Krainc, 2017).

The current therapeutic gold standard for the motor symptoms is the administration of levodopa, which only temporarily restores striatal dopamine levels (Cotzias et al., 1974; Lloyd et al., 1975). Other treatment options include deep brain stimulation and a variety of pharmacotherapies (Benabid et al., 1993; Tolosa et al., 1998; Vercueil et al., 1998). Due to the inefficiency of the current pharmacological and surgical approaches, gene therapy, especially viral vector mediated therapy, has been explored. Adeno-associated viruses (AAVs) are the most commonly used vectors in pre-clinical and clinical studies due to their low toxicity, negligible inflammatory responses, sustained transgene expression and a plethora of capsid serotypes (McCown, 2005).

Generating animal models that replicate both the α -synucleinopathy and the progressive development of motor symptoms still is a challenge. Overexpression of α -synuclein using AAVs is a promising strategy as α -synuclein overexpression in rats mimics endpoints of the human disease in a progressive manner suitable to test therapeutic interventions

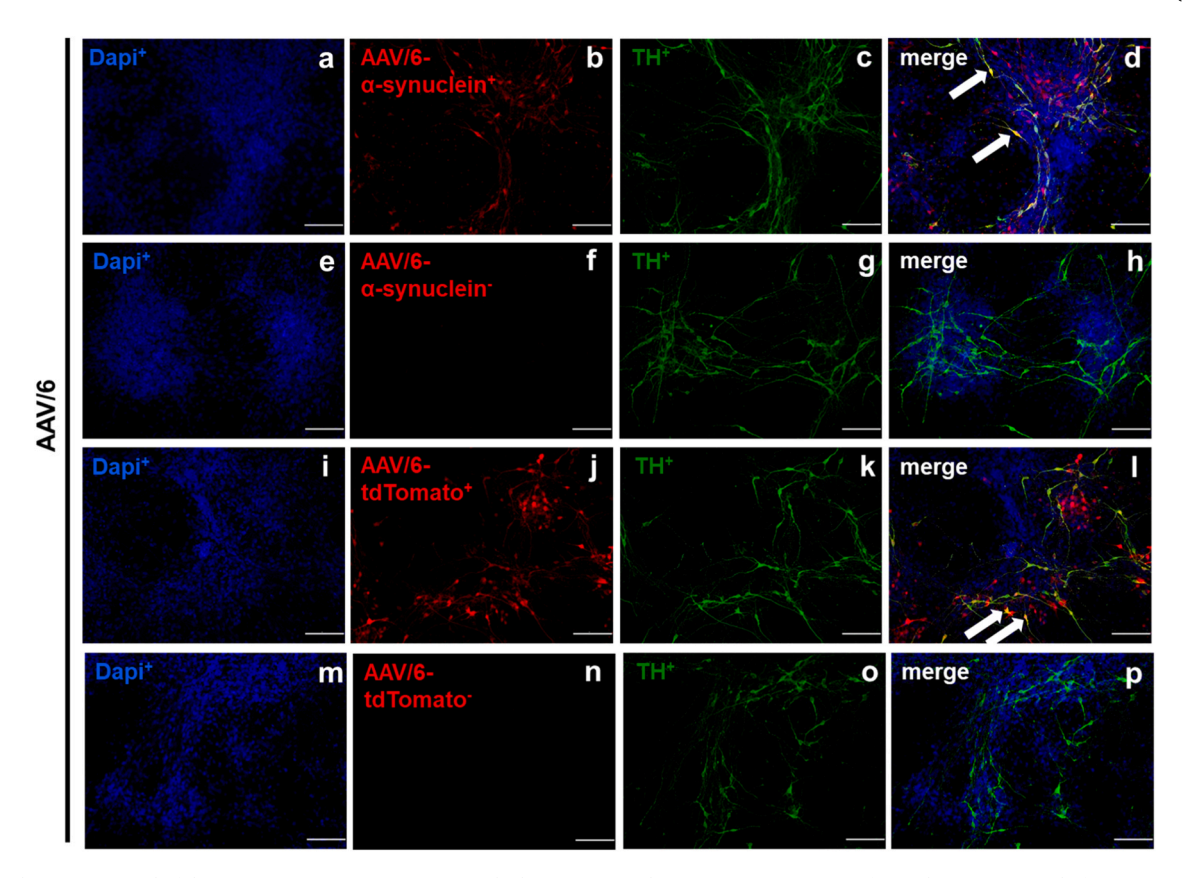


Fig. 2. Transduction potential of the AAV/6 serotype overexpressing the human α -synuclein protein. Assessment of transduction potential of AAV/6- α -synuclein and AAV/6-tdTomato in primary DA neurons. 80.000 cells were seeded per well and differentiated for 3 days. After 3 DIV, cells were transduced with 1×10^{10} vg/μL AAV/6- α -synuclein or AAV/6-tdTomato for 3 days, respectively. After 8 DIV, cells were fixed and stained for TH (green) and Dapi (blue). AAV/DJ- α -synuclein transduced cells were additionally stained for α -synuclein (red), while fluorescence of tdTomato (red) in AAV/DJ-tdTomato transduced cells was directly visualized without additional staining. Representative immunocytochemical stainings of DA neurons transduced with AAV/6- α -synuclein (a-d), AAV/6-tdTomato (i-l) and control DA neurons with no viral transduction (AAV/6- α -synuclein (e-h) and AAV/6-tdTomato (m-p), respectively). White arrows point towards transduced TH⁺ cells (d and l). All images were acquired with a 20 × magnification objective. Scale bar is 100 μm.

(Azeredo da Silveira et al., 2009; Kirik et al., 2002).

In a previous study, we established an AAV2/DJ- α -synuclein-based model for PD, which demonstrated pre-symptomatic and early symptoms, but did not exhibit a progressive motor phenotype (von Hövel et al., 2019). Thus, within this study, we aimed to develop a refined viral model of PD that closely mimics the full range of neuropathological symptoms of the disease. This includes resistant α -synuclein inclusions, early-stage inflammation, progressive loss of dopaminergic neurons, and, most importantly, a gradual, progressive motor impairment. The goal was to generate a model that provides a therapeutic window, allowing the evaluation of potential treatments over the course of disease progression.

2. Materials and methods

2.1. Ethics statement

All surgical procedures, animal experiments and euthanasia were conducted in strict accordance with the German Animal Welfare Act and were approved by the Lower Saxony State Office for Consumer Protection and Food Safety (LAVES, Hannover, Germany; reference number 33.12–42502–04–21/3676 and §4 notification according to the German Welfare Act).

2.2. Animals

All rats were housed in Macrolon Type IV S open cages (Techniplast, Hohenpeissenberg, Germany) in groups of maximum 4 animals and kept

under controlled environmental conditions $(22\pm2^{\circ}\text{C}, 55\pm10\,\%$ humidity) with a 14 h light-10h dark cycle. Animals received normal diet (1324 TPF from Altromin Spezialfutter GmbH & Co. KG, Lage, Germany) and tap water *ad libitum*. Wood chip bedding (Espentiereinstreu AB P3, AsBe-wood GmbH; Gransee, Germany) and nesting material Enviro-dri® (Claus GmbH, Limburgerhof, Germany) were provided. Adult female Sprague Dawley rats were purchased from Janvier (Rte du Genest, France) weighting 225–250 g at the start of the experiments. Only female rats were examined in order to maintain comparability to our previous study (von Hövel et al., 2019). For *in vitro* experiments, pregnant Sprague Dawley rats were purchased from Charles River (Sulzfeld, Germany).

2.3. Primary DA progenitor cells

Primary DA progenitor cells were obtained by euthanizing pregnant Sprague Dawley rats on embryonic day 12 (E12). Embryos were isolated and ventral mesencephala (VM) dissected to generate a cell suspension of primary DA progenitor cells (Björklund et al., 1983; Nikkhah et al., 2009; Timmer et al., 2006). Generated VM were incubated for 20 min in preparation medium and afterwards treated with attachment medium (3 % fetal calf serum). Cell suspension was centrifuged for 5 min at 1000 rpm and resuspended in attachment medium to obtain a single cell suspension. Cell viability was determined by trypan blue dye (Sigma-Aldrich, Munich, Germany) exclusion by means of a Neubauer chamber (Marenfeld, Lauda-Königshofen, Germany).

Primary DA progenitor cells were generated as previously described (Timmer et al., 2006). Briefly, 500.000 cells/well were seeded on

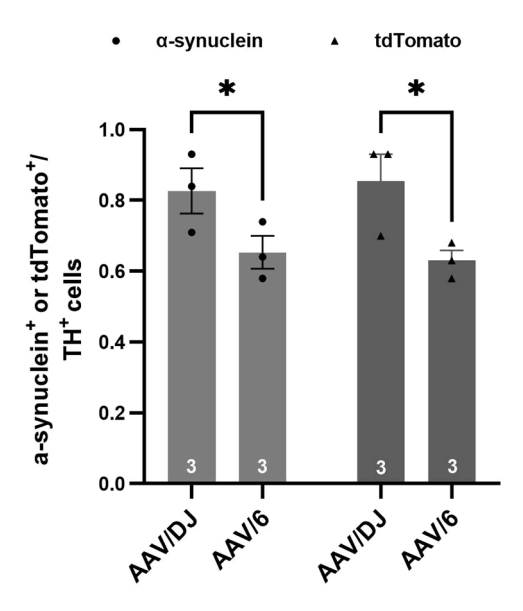


Fig. 3. Transduction efficiency of AAV/DJ and AAV/6 serotype overexpressing the human α-synuclein protein. Assessment of transduction efficiencies of AAV/DJ-α-synuclein, AAV/DJ-tdTomato, AAV/6-α-synuclein and AAV/6-tdTomato in primary DA neurons. 80,000 cells were seeded per well and differentiated for 3 days. After 3 DIV, cells were transduced with 1×10^{10} vg/μL AAV/DJ-α-synuclein, AAV/DJ-tdTomato, AAV/6-α-synuclein or AAV/6-tdTomato for 3 days, respectively. After 8 DIV, cells were fixed and stained for TH (green), Dapi (blue), α-synuclein (red) or against tdTomato (red), respectively. Quantitative estimation of double positive cells (α-synuclein⁺/TH⁺ or tdTomato⁺/TH⁺) of 3 independent experiments. Higher transduction efficiency of the AAV/DJ serotype (for both α-synuclein and tdTomato viral constructs) compared to the AAV/6 serotype. Data are represented as mean \pm SEM (repeated measurements). Two-way ANOVA followed by Tukey's post hoc analysis with *p < 0.5.

fibronectin/polyornithine (0.1 mg/mL) coated wells in attachment medium. The following day, medium was replaced with proliferation medium and cells were incubated for 3 days. After 4 days *in vitro* (DIV), cells were detached for 3 min by using trypsin (GibcoTM, life technologies, Warrington, UK) and the reaction was stopped by adding attachment medium containing 0.05 % DNase (Roche, Basel, Switzerland). Cells were incubated in proliferation medium consisting of 10 % fetal calf serum (GibcoTM, life technologies, Warrington, UK) and 10 % dimethyl sulfoxide (Sigma-Aldrich, Munich, Germany) and stored in liquid nitrogen at $-196^{\circ}\mathrm{C}$. Medium compositions were used as previously described (Ratzka et al., 2012).

2.4. Viral transduction of primary DA neurons

Eighty thousand (80.000) cells/well were plated on 24-well plates (glass, Ø 13 mm, VWR, Darmstadt, Germany) containing coverslips precoated with fibronectin/polyornithine (0.1 mg/mL; Sigma-Aldrich, Munich, Germany). Cells were seeded in attachment medium for one day. The following day, cells were cultured in differentiation medium for 3 days. After 4 DIV, DA neurons were transduced with 1 μL of either AAV/DJ- α -synuclein, AAV/DJ-tdTomato, AAV/6- α -synuclein or AAV/6-tdTomato (engineered by VectorBuilder, Chicago, USA) in differentiation medium in a titer of 1 \times 10 10 vg/ μL for 3 days. AAV/DJ- α -synuclein and AAV/6- α -synuclein each contained a transgene cassette overexpressing the human SNCA. AAV/DJ-tdTomato and AAV/6-tdTomato, each contained a red fluorescent tdTomato protein.

2.5. Immunocytochemistry

Cells were fixed with 4% paraformaldehyde (PFA, Sigma-Aldrich,

Munich, Germany) in 1xPBS for 20 min, washed thrice with 1 ×PBS and blocked for 30 min at room temperature in 1 ×PBS containing 0.3 % TritonX-100 (Roche, Basel, Switzerland), 3 % normal goat serum (NGS, 16210-064, GibcoTM, life technologies, Warrington, UK) and 5% bovine serum albumin (BSA, A9418, Sigma-Aldrich, Munich, Germany). After blocking, primary antibodies rabbit anti-tyrosine hydroxylase (1:1000; AB152, Millipore, Darmstadt, Germany) and mouse antiα-synuclein (1:200; SC12767, Santa Cruz Biotechnology, Heidelberg, Germany) were added. The mouse anti-α-synuclein antibody (SC12767) targets with high-specificity the amino acids 121-125 of human origin. Primary antibodies were incubated over night at 4°C in 1×PBS containing 0.3 % TritonX-100, 3 % BSA and 1 % NGS. The next day, cells were washed thrice with 1 ×PBS. Secondary antibodies AlexaFluor 488 anti-rabbit (1:500, Invitrogen, Darmstadt, Germany) and AlexaFluor 555 anti-mouse (1:1000, Invitrogen, Darmstadt, Germany) in 1 ×PBS containing 0.3 % TritonX-100 and 1 % NGS were added for one hour. After incubation, cells were washed thrice with 1 × PBS and stained with 4',6-Diamidin-2-phenylindol (1:1000; Sigma-Aldrich, Munich, Germany) in 1 × PBS. Visualization took place by use of fluorescence microscopy (BX61; Olympus Deutschland GmbH, Hamburg, Germany). Image acquisition was performed with Cell F and CellSens Dimensions Ink. Software (Olympus Deutschland GmbH, Hamburg, Germany) using a $20 \times \text{objective}$ and a numerical aperture of 0.17.

2.6. Protein quantification

For protein quantification, cells were seeded and cultured on 6-well dishes (Nunc, Fischer Scientific, Schwerte, Germany) and transduced as already described (2.4 viral transduction of primary DA neurons). After viral transduction, cells were incubated with 0.005 % trypsin (GibcoTN, life technologies, Warrington, UK) in differentiation medium for 3 min. The reaction was stopped by adding attachment medium containing 0.05 % DNase (Sigma, Taufkirchen, Germany). For each sample, two wells were pooled and centrifuged thrice at 20.000 rpm. Cell pellets were lysed in radioimmune precipitation assay (RIPA) buffer consisting of 137 mM sodium chloride (J.T. Baker, Schwerte, Germany), 20 mM tris-hydrochloride (Sigma, Taufkirchen, Germany) pH 7, 525 mM β-glycerolphosphate (Sigma, Taufkirchen, Germany), 2 mM ethylendiaminetetraacetic acid (Sigma, Taufkirchen, Germany), 1 mM sodium orthovanadate (Sigma, Taufkirchen, Germany), 1 % (w/v) sodium desoxycholate (Sigma, Taufkirchen, Germany) and 1 % (v/v) TritonX-100 containing phosphatase inhibitor (Roche, Mannheim, Germany) and protease inhibitor (Roche, Mannheim, Germany). Per sample, 50 µg protein were dissolved in Laemmli buffer [25 mM tris-hydrochloride pH 8, 7.5% sodium dodecyl sulfate, 25% glycerol, 12.5% β-mercaptoethanol, 0.5% bromphenol blue (Sigma, Taufkirchen, Germany)] and denaturized by boiling at 90°C for 15 min. Protein samples were separated by sodium dodecyl sulfate-polyacrylamide gel electrophoresis and tracked by a broad range protein ladder (Merck, Darmstadt, Germany). Proteins were transferred on an Amersham Protran Premium nitrocellulose blotting membrane [0.45 µm; Healthcare, (Th. Greyer), Hamburg, Germany]. After the transfer, membranes were blocked for 30 min in blocking solution consisting of 5 % BSA in tris-buffered saline [TBS containing 0.03 % (v/v) Tween buffer (Sigma, Taufkirchen, Germany]. Primary antibodies goat anti-tdTomato (1:500; MBS448092, MyBio-Source, Eersel, Netherlands) and mouse anti-glyceraldehyd-3phosphate-dehydrogenase (GAPDH, 1:1000; Cell signaling, Leiden, Netherlands) were incubated overnight at 4°C. Secondary antibodies (anti-mouse horseradish peroxidase (HRP)-linked whole antibody [1:4000; GE Healthcare, (Th. Greyer), Hamburg, Germany] and antirabbit HRP-linked whole antibody [1:5000; GE Healthcare, (Th. Greyer)] were incubated in 5 % milk powder (Heirler Cenovis, Radolfzell, Germany) for 1 h at room temperature. Bands were visualized by INTAS Science Imaging (Göttingen, Germany), and densitometric analyses were performed by LabImage1D Software (Göttingen, Germany).

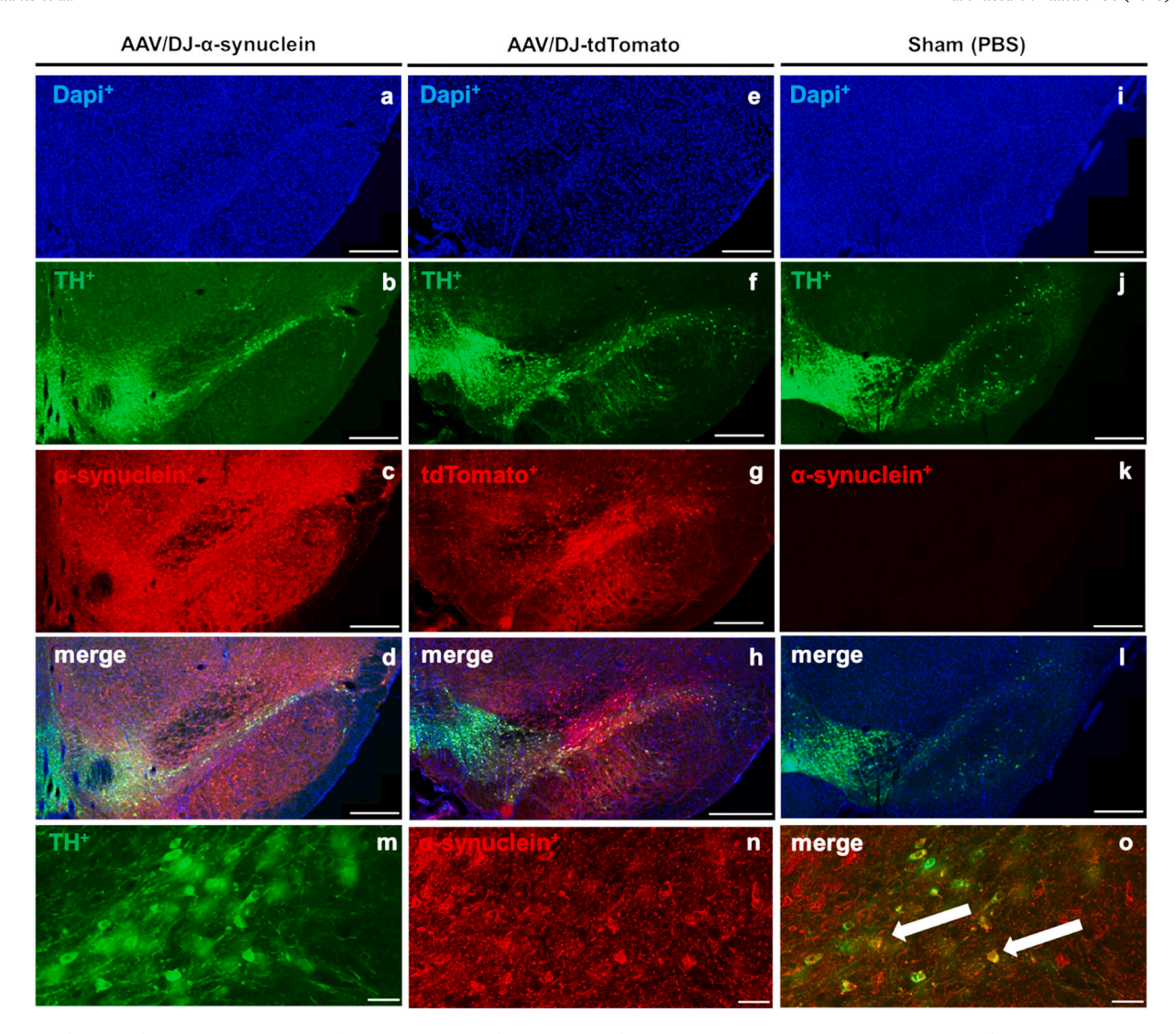


Fig. 4. Transduction of DA neurons in SNpc after AAV/DJ- α -synuclein, AAV/DJ-tdTomato or 1 ×PBS injection. Representative fluorescence staining of nuclei (Dapi⁺), remaining TH⁺ neurons and transduced cells located in the SNpc after AAV/DJ- α -synuclein (a-d) and AAV/DJ-tdTomato injection (e-h) at 12 weeks, respectively, or after 1 ×PBS injection at 8 weeks (i-l). Exemplary staining of α -synuclein-transduced TH⁺ cells after AAV/DJ- α -synuclein injection at 12 weeks; white arrows point towards transduced cells (m-o). All images were acquired with a 20 × (a-l) or 40 × (m-o) magnification objective. Scale bar is 500 μm (a-l) or 50 μm (m-o).

2.7. Stereotaxic injections

All rats received a unilateral stereotaxic injection into the right SNpc (AP -5.2 mm, LAT -2.0 mm, DV -7.2 mm) with reference to individual bregma and dura coordinates (Paxinos and Watson, 2013). At the time of the injection the animals were 110-155 days old. Injection was performed under general anaesthesia with isoflurane (induction: 5 % in O₂, maintenance: 2-3% in O2 CP Pharma, Burgdorf, Germany). Prior to surgery, analgesia was administered via subcutaneous (s.c.) injection of 5 mg/kg body weight carprofen (carprosol, 50 mg/mL, CP Pharma, Burgdorf, Germany), which was further administered for 3 consecutive days after surgery. Additionally, Emla® creme (25 mg/g lidocaine + 25 mg/g prilocaine, Aspen, Munich, Germany) was administered to the shaved head for local anesthesia before dermal incision. After disinfection and dermal incision, a few drops of 1 % lidocaine (xylocaine, Aspen, Munich, Germany) were applied to the skull for local anesthesia of the periost. Animals were fixed in a stereotaxic frame (Harvard Apparatus, Holliston, USA) and viral constructs overexpressing the human SNCA, the red fluorescent tdTomato protein or sham (no viral construct; only 1xPBS injected) were applied with an UltraMicroPump microsyringe injector (World Precision Instruments, Sarasota, USA) using a $10\,\mu L$ gastight syringe with a 33 gauche needle (1701 small hub Hamilton, Carl Roth, Karlsruhe, Germany). Injection rate was 0.3 µL/min. After injection, the needle was not withdrawn for 5 min to ensure sufficient diffusion of the injected solution. The wound was closed with $11 \times 2 \text{ mm}$ wound clips (BN511, Braun, Melsungen, Germany). After surgery, animals received a s.c. injection of 5 mL 0.9 % saline (Braun, Melsungen, Germany) and were closely monitored until regaining full consciousness. Seventy-one rats received an injection of either 3 µL AAV/DJ- α -synuclein (1 ×10¹⁰ vg/ μ L), 3 μ L AAV/DJ-tdTomato (1 ×10¹⁰ vg/μL) or 3 μL 1 × PBS (sham operated animals). One animal was excluded due to respiratory complications during anaesthesia because of a brain tumor. Out of 70 operated animals, further 11 were excluded from stereological, densitometric and behavioral evaluation due to misinjections in close proximity to the SNpc, verified post mortem by histological evaluation. Animals were randomly allocated to the injection groups by means of Random Team Generator (www.randomlists. com/team-generator).

2.8. Behavioral assessment

A battery of three different behavioral tests (cylinder, stepping and

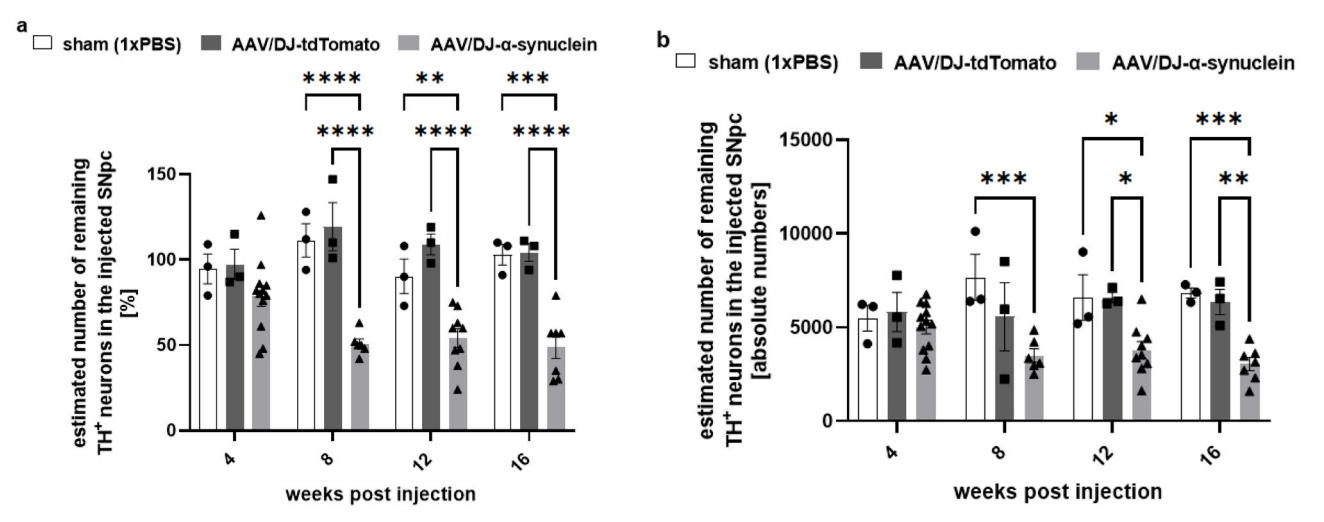


Fig. 5. Stereological evaluation of DA neurons in SNpc. Quantification of percentages of remaining TH $^+$ neurons in the injected SNpc (normalized to the non-injected hemisphere of each rat) revealed loss of DA neurons at 8 (n = 6), 12 (n = 9) and 16 (n = 7) weeks post AAV/DJ- α -synuclein injection compared to sham (1 × PBS; n = 3) or AAV/DJ-tdTomato (n = 3) operated rats (a). Quantification of absolute numbers of remaining TH $^+$ neurons in the injected SNpc revealed loss of DA neurons at 8 (n = 6), 12 (n = 9) and 16 (n = 7) weeks post AAV/DJ- α -synuclein injection compared to sham (1 × PBS; n = 3) or AAV/DJ-tdTomato (n = 3) operated rats (b). No loss of DA neurons in the injected SNpc at 4 weeks post AAV/DJ- α -synuclein (n = 12) injection compared to sham (1 × PBS; n = 3) or AAV/DJ-tdTomato (n = 3) operated rats. Data are represented as mean \pm SEM. Two-way ANOVA followed by Tukey's post hoc analysis with *p < 0.5, **p < 0.01, ***p < 0.001 and ****p < 0.0001.

staircase test) were performed after a two-week training and acclimatization period pre injection (baseline) and then 4-, 8-, 12- and 16 weeks post injection. All 3 tests were conducted over a period of 13 days per timepoint. The experimenter and analyst was blinded to the experimental conditions.

For the cylinder test, a transparent glass cylinder was placed in front of two mirrors to assess forelimb asymmetry while rearing (Schallert et al., 2000). Animals were recorded over a total timeframe of 5 min, during which the first 20 wall touches of the cylinder were counted. Use of the left paw is expressed as the % of the spontaneous first 20 limb uses (both forepaws) towards the walls of the glass cylinder while rearing.

Forelimb akinesia was further evaluated by the stepping test (Olsson et al., 1995) on 3 consecutive days (twice daily). Animals were positioned in a horizontal plane above the flat surface of a table while loosely fixing both hindlimbs as well as one of the forelimbs (the one not evaluated). The animal was moved sideways (forehand and backhand direction approx. 90 cm) over a period of 5 sec while the forelimb kept contact with the surface of the table enabling the animal to perform steps. Adjusting steps of each forelimb in each direction were counted. The mean number of steps performed over 3 consecutive days in both trials per day was calculated.

Fine motor skills (ability to reach, grasp and retract food pellets) were evaluated in both forelimbs independently and monitored over 15 min with the staircase test (Montoya et al., 1991). A double staircase with seven steps on each side was loaded with food pellets (four per step) (Dustless Precision Pellets, 45 mg, chocolate flavour, Bio-Serv, Flemington, USA). Rats underwent a food-restricted period during the test to increase their motivation. During the whole test period (acclimatization and actual test), the feeding schedule was changed from *ad libitum* access to 12–15 g of chow per animal per day (fed in the evening). During the testing period, rats were placed into the staircase boxes and after 15 min, the number of remaining pellets on each stair was counted on both sides. The test was repeated over 6 consecutive days after a 4-day acclimatization period to the test box for each timepoint. The mean number of pellets grasped on both sides (left is contralateral to lesion) of the staircase box over 6 days was calculated.

2.9. Perfusion and immunohistochemistry

Rats were perfused 4-, 8-, 12- or 16 weeks post injection as previously

described (Rumpel et al., 2015). Briefly, rats were euthanized using CO_2 inhalation and transcardially perfused with 250 mL 0.9 % saline followed by 250 mL 4 % PFA (Sigma-Aldrich, Munich, Germany). Brains were isolated and post-fixed overnight at 4°C. The following day, brains were transferred to 30 % sucrose (Roth, Karlsruhe, Germany) for cryoprotection and embedded in ethylene glycol (Merck, Karlsruhe, Germany) and glycerol (Roth, Darmstadt, Germany). After frozen at -20° C, brains were coronally sectioned on a freezing stage microtome (Leica Biosystems, Wetzlar, Germany) at a 40 μ m thickness in a series of 6.

Immunohistochemical stainings were conducted on free-floating sections. For fluorescent stainings, sections were blocked for one hour in 5 % BSA (A9418, Sigma-Aldrich, Munich, Germany) blocking solution (1 \times PBS). Every third section was used for double immunofluorescence staining with rabbit anti-tyrosine hydroxylase (TH, 1:500, AB152, Millipore, Darmstadt, Germany) in 1 % NGS (16210-064, GibcoTM, life technologies, Warrington, UK) and 0.3% TritonX-100 (Roche, Basel, Switzerland) in $1 \times PBS$ and either mouse anti- α -synuclein (1:200: SC12767, Santa Cruz Biotechnology, Heidelberg, Germany) or goat antitdTomato (1:200; MBS448092, MyBioSource, Eersel, Netherlands) in 1 % BSA (A9418, Sigma-Aldrich, Munich, Germany) and 0.3 % TritonX-100 (Roche, Basel, Switzerland) in 1 × PBS overnight. The mouse antiα-synuclein antibody (SC12767) targets with high-specificity the amino acids 121-125 of the human sequence. Additional series were stained with mouse anti-TH (1:500, T1299, Sigma-Aldrich, Munich, Germany) and rabbit anti-glial fibrillary acidic protein (GFAP, 1:400; 9269, Sigma-Aldrich, Munich, Germany), rabbit anti-calbindin D-28k (1:4000; CD 38, Swant, Burgdorf, Switzerland) or rabbit anti-Kir 3.2 (Girk2, 1:400; APC-006, Almone, Jerusalem, Israel) in 1 % BSA (A9418, Sigma-Aldrich, Munich, Germany) and 0.3 % TritonX-100 (Roche, Basel, Switzerland) in $1 \times PBS$ overnight. The following secondary antibodies were used: Alexa Fluor 555 anti-mouse (1:500; Invitrogen, Darmstadt, Germany), Alexa Fluor 488 anti-mouse (1:500; Invitrogen, Darmstadt, Germany), Alexa Fluor 555 anti-rabbit (1:500; Invitrogen, Darmstadt, Germany), Alexa Fluor 488 anti-rabbit (1:500; Invitrogen, Darmstadt, Germany), Alexa Fluor 555 anti-goat (1:500; Invitrogen, Darmstadt, Germany) and Alexa Fluor 488 anti-goat (1:500; Invitrogen, Darmstadt, Germany) in 1 % BSA (A9418, Sigma-Aldrich, Munich, Germany) and 0.3 % TritonX-100 (Roche, Basel, Switzerland) in 1 × PBS overnight. To visualize cell nuclei, a Dapi staining (1:1000, Sigma-Aldrich, Munich, Germany) was added. Moreover, one series of each brain was stained with the primary

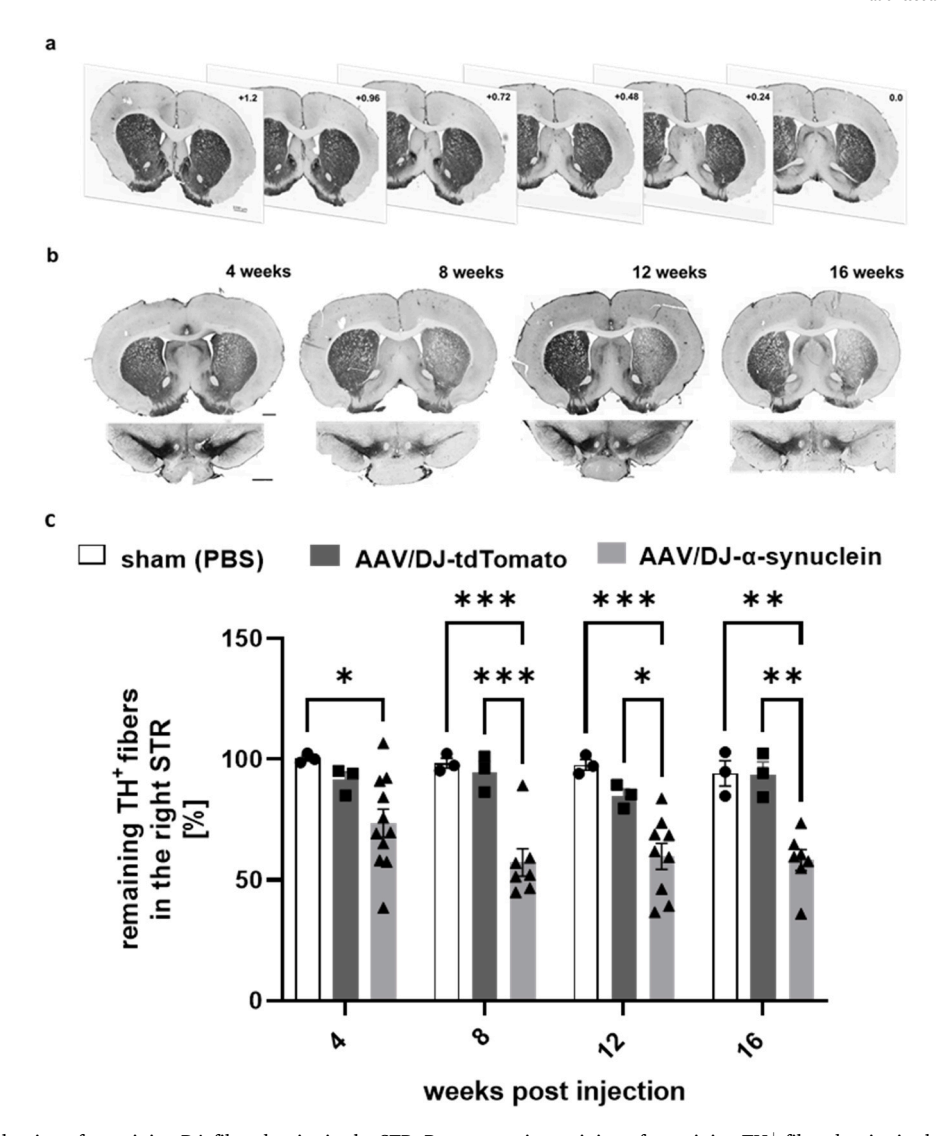


Fig. 6. Densitometric evaluation of remaining DA fiber density in the STR. Representative staining of remaining TH $^+$ fiber density in the STR at serial sections of 6 different rostrocaudal striatal planes (AP: +1.2; +0.96; +0.72; +0.48; +0.24 and 0.0 relative to bregma) of a sham (1 ×PBS) operated animal (a). Representative staining of remaining TH $^+$ fiber density in the STR (+0.48 relative to bregma) and of remaining TH $^+$ cells located in the SNpc (-5.04 relative to bregma) 4, 8, 12 and 16 weeks post AAV/DJ-α-synuclein injection (b). All images were acquired with a 20 × magnification objective. Scale bar is 1000 μm. Quantification of percentages of remaining TH $^+$ fiber density in the STR revealed loss of DA fibers at 4 (n = 11), 8 (n = 7), 12 (n = 9) and 16 (n = 7) weeks post AAV/DJ-α-synuclein injection compared to sham (1 × PBS; n = 3) or AAV/DJ-tdTomato (n = 3) operated rats (c). Data are represented as mean ± SEM. Two-way ANOVA followed by Tukey's post hoc analysis with *p < 0.5, **p < 0.01 and ***p < 0.001.

antibody mouse anti-TH (1:500, T1299, Sigma-Aldrich, Munich, Germany) followed by avidin-biotin-complex (ABC) kit (Vector Laboratories, Petersborough, UK) with biotinylated rabbit anti-mouse antibody (1:200, Dako, Glostrup, Denmar) and 3,3'-diaminobenzidine (DAB, Sigma-Aldrich, Munich, Germany) with ammonium nickel sulfate intensification for visualization. Sections were digitized and visualized with an AxioScan.Z1 (Zeiss Microscopy, Oberkochen, Germany) slide scanner and the Zen2011 software (Zeiss Microscopy, Oberkochen, Germany).

Iba1 analyses were performed in a collaborating laboratory as follows: free-floating sections were washed thrice in 0.05 M PBS for 10 min and blocked in 10 % NGS in TBS. Incubation with primary antibody staining solution took place overnight at 4°C [2 % NGS/0.5 % Triton X in TBS; guinea-pig anti-Iba1 (#234308, 1:500, Synaptic systems, Göttingen, Germany), mouse-anti-TH (#22941, 1:2000, Immunostar, Hudson, Wisconsin, USA)]. Afterwards, sections were washed thrice with 0.05 M TBS for 10 min and incubated with secondary antibodies (Invitrogen, goat-anti-guineapig AF647 and goat-anti-mouse AF488) in

5 % NGS for one hour. Slices were mounted and coverslipped with Prolong Gold Antifade DAPI medium (#P36931, Invitrogen, Waltham, Massachusetts, USA). Images were acquired with a Zeiss AxioObserver Setup with a Calibri 7 LED (Carl Zeiss, Oberkochen, Germany) light source and Zen Blue Pro 2.6 Software.

For staining against S129-phosporylated α -synuclein, sections were washed twice in 10 mM TBS (Tris-HCl) for 5 min and once in 10 mM TBS containing 0.05 % Tween (pH 7.8; 100 mM NaCl) for 5 min. Afterwards, sections were incubated with 20 µg/mL proteinase K (#03115879001, Roche, Mannheim, Germany) in 10 mM TBS containing 0.1 % Tween for 45 min. Sections were washed twice in 10 mM TBS for 5 min and once in 1 ×PBS for 5 min. In addition, sections were incubated with a solution consisting of 3 % hydrogen peroxide (Merck, Darmstadt, Germany), 10 % methanol (J.T. Baker, Schwerte, Germany) and 1 ×PBS for 10 min. After incubation, sections were washed trice in 1 ×PBS for 5 min. Incubation with primary antibody staining solution took place overnight (1:2000; AB59264, Abcam, Cambridge, United Kingdom). Sections were washed thrice in 1 ×PBS for 5 min and incubated with biotinylated goat

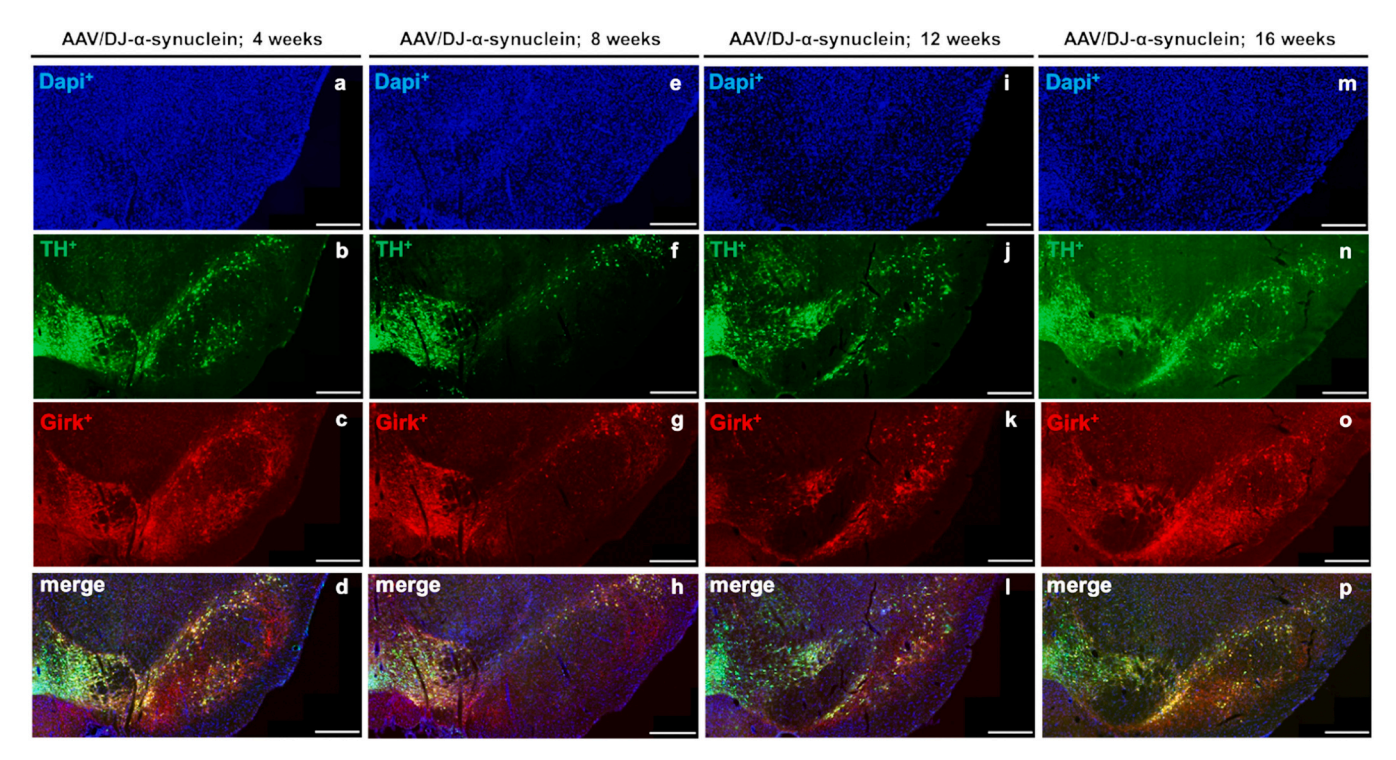


Fig. 7. Progressive degeneration of $Girk^+$ DA neurons in the VTA and SNpc at different timepoints after AAV/DJ-α-synuclein injection. Representative fluorescence staining of nuclei (Dapi⁺), remaining TH^+ neurons (green) and $Girk^+$ DA neurons (red) located in the SNpc and the VTA after AAV/DJ-α-synuclein injection at 4 (a-d), 8 (e-h), 12 (i-l) and 16 weeks (m-p). All images were acquired with a $20 \times magnification$ objective. Scale bar is $500 \ \mu m$.

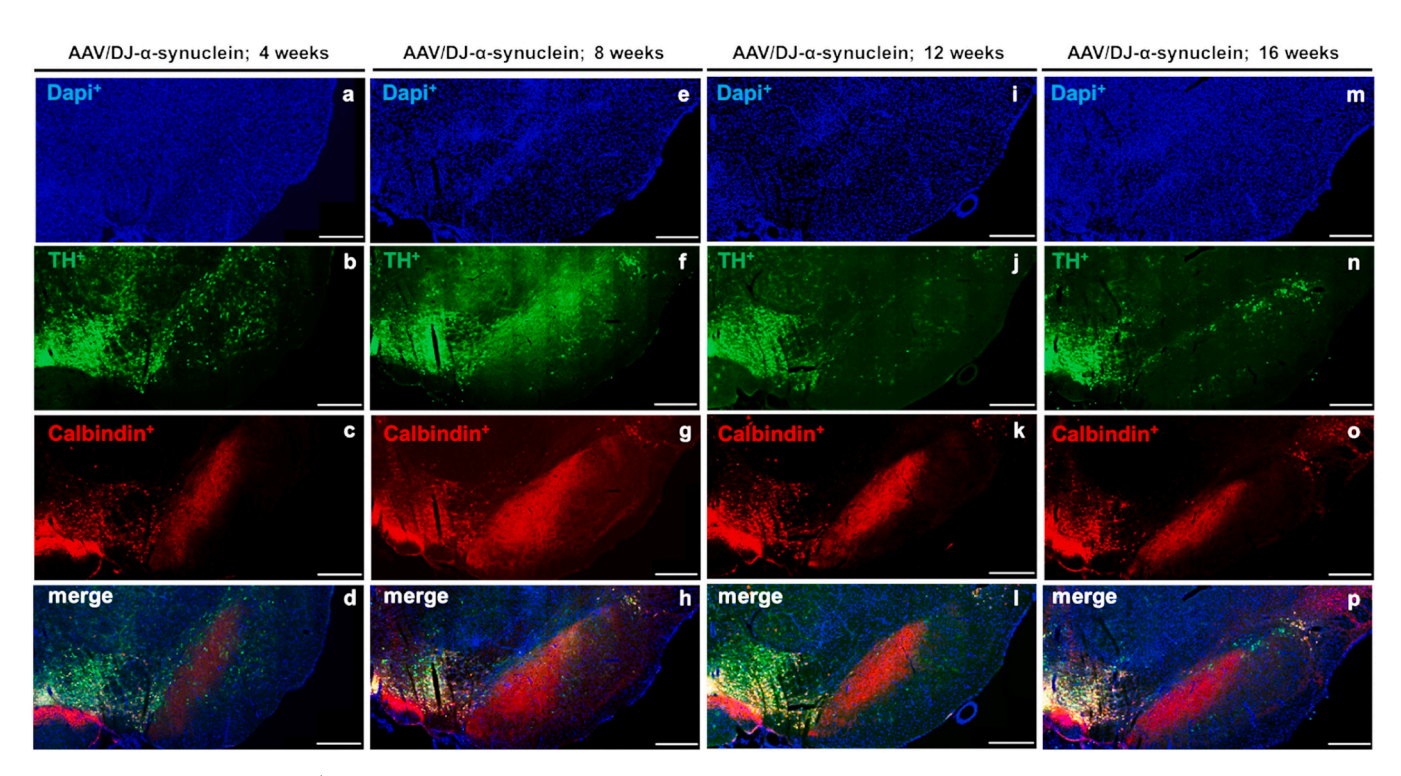


Fig. 8. No differences in Calbindin $^+$ DA neurons in the VTA and the lateral tier of the SNpc at different timepoints after AAV/DJ- α -synuclein injection. Representative fluorescence staining of nuclei (Dapi $^+$), remaining TH $^+$ neurons (green) and Calbindin $^+$ DA neurons (red) located in the SNpc and the VTA after AAV/DJ- α -synuclein injection at 4 (a-d), 8 (e-h), 12 (i-l) and 16 weeks (m-p). All images were acquired with a 20 × magnification objective. Scale bar is 500 μm.

anti-rabbit antibody (1:200; Jackson Immunoresearch, Dianova, Hamburg, Germany) for one hour. Sections were washed thrice in $1\times PBS$ for 5 min and incubated with avidin-biotin complex ABC kit (Vector Laboratories, Peterborough, UK) and DAB (Sigma Adrich,

Munich, Germany) with ammonium nickel sulfate (Honeywell Riedel de Haen, Seelze, Germany) intensification. All images were visualized by AxioScan.Z1 (Zeiss Microscopy, Oberkochen, Germany) slide scanner and Zen2011 software (Zeiss Microscopy, Oberkochen, Germany).

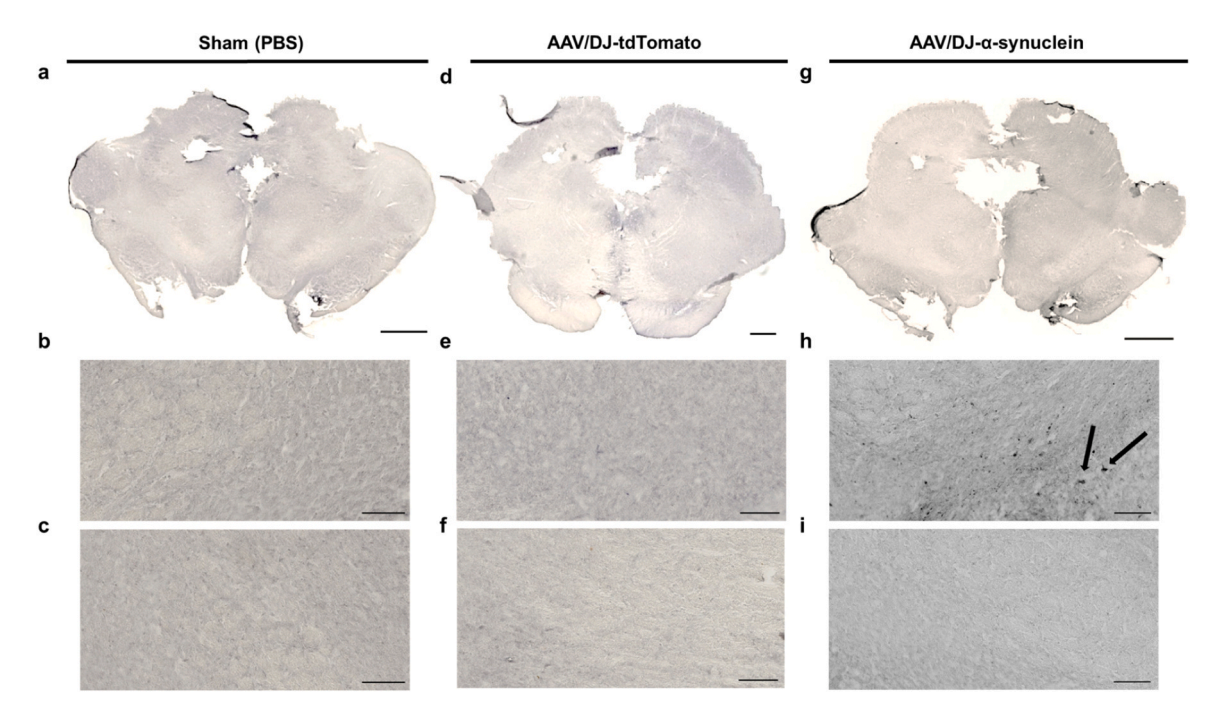


Fig. 9. Formation of proteinase K resistant S129-phosphorylated human α-synuclein protein inclusions after AAV/DJ- α -synuclein, AAV/DJ-tdTomato or 1 ×PBS injection. Representative staining of the injected hemisphere relative to the non-injected hemisphere after AAV/DJ- α -synuclein, AAV/DJ-tdTomato or 1 ×PBS injection at 16 weeks post injection (a, d and g). Representative staining of the injected hemisphere (b) relative to the non-injected hemisphere (c) in sham (1 ×PBS) operated rats at 16 weeks post injection. Representative staining of the injected hemisphere (e) relative to the non-injected hemisphere (f) at 16 weeks post injection with AAV/DJ-tdTomato. Representative staining of the injected hemisphere (h) relative to the non-injected hemisphere (i) at 16 weeks post injection with AAV/DJ-α-synuclein; black arrows point towards proteinase K resistant phosphorylated α-synuclein inclusions in the injected SNpc. All images were acquired with a 40 × magnification objective (a-i). Scale bar is 1000 μm (a and g), 500 μm (d) or 100 μm (b, c, e, f, h and i).

2.10. Stereological and densitometric evaluation

Evaluation of the total number of DA neurons in the SNpc was conducted by stereological estimation. Every third section was analyzed by means of the optical fractionator workflow of Stereo Investigator software (MBF Bioscience, Vermont, USA) using a 40 × objective and a numerical aperture of 0.17. The whole area of the SNpc (excluding the dorsal part) was counted, which encompassed 20–24 sections per animal, using a grid size of $200\times200~\mu\text{m}$, a counting frame of $110\times110~\mu\text{m}$ and a $22~\mu\text{m}$ dissector height with a 2 μm guard zone distance. Tissue thickness was determined at each counted section. The accepted coefficient of error was <0.08 (Gundersen m=1). The experimenter and analyst was blinded to the experimental conditions.

Striatal fiber density was evaluated by densitometric analysis by a blinded experimenter as previously described (Rumpel et al., 2015). The optical density of the STR of both hemispheres was measured on brain sections stained for TH at six coronal levels: AP $+1.2,\,+0.96,\,+0.72,\,+0.48,\,+0.24,\,0.0$ mm relative to bregma (Paxinos and Watson, 2013) using ImageJ software (National Institute of Health, Bethesda, USA). The optical density of the corpus callosum was set as the background and therefore, was subtracted from the values. Results are expressed as % of remaining fibers within the lesioned right STR relative to the contralateral STR.

Iba1 data was evaluated using ImageJ with Iba1 $^+$ cells manually counted (Cell counter plugin) in a standardized ipsi- and contralateral SNpc 20x magnification field in AAV/DJ- α -synuclein treated animals. Additionally, the mean fluorescence intensity of the Iba1 channel was measured.

2.11. Statistical analyses

All statistical analyses were performed with GraphPad Prism software, version 9 (GraphPad Software Inc., San Diego, CA). Results are

presented as mean \pm SEM. Paired students t-test, ordinary one-way or two-way ANOVA was applied for comparisons between groups (repeated measurements or not), followed by multiple comparisons post-hoc tests (Turkey's or Dunnett's) as indicated. Differences were considered significant in case of a p-value < 0.05 and represented as follows: *: p-value < 0.05, **: p-value < 0.01, ***: p-value < 0.001 and ****p < 0.0001.

3. Results

3.1. Evaluation of the AAV/DJ and AAV/6 serotypes in primary DA neurons in vitro

We previously showed that the AAV2/DJ serotype is able to transduce DA neurons *in vivo* and that transduction achieved by stereotaxic injection of two different viral constructs (wildtype- or E46K human *SNCA* encoding for α -synuclein) leads to degeneration of DA neurons located in the SNpc (von Hövel et al., 2019). We also showed that loss of DA neurons and their fibers results in behavioral deficits. To establish a refined rat model closer mimicking both the histological and behavioral hallmarks of PD, we first evaluated the transduction efficiencies of 4 different AAV serotypes overexpressing the human α -synuclein protein in primary DA neurons *in vitro* (AAV/5 and AAV/9 data not shown as no transduction was evident).

3.1.1. Higher transduction efficiency of the AAV/DJ serotype in primary DA neurons

Transduction efficiency was assessed by immunocytochemically staining DA neurons (TH $^+$) to identify successful viral transduction. We used viral constructs overexpressing either the human α -synuclein or the red fluorescent tdTomato protein. The assessment was performed for both the AAV/DJ and the AAV/6 serotypes. Double positive DA neurons were counted. Exemplary stainings for all conditions (control: no viral

AAV/DJ-α-synuclein non-injected SNpc a TH d injected SNpc a TH d b lba1 e b lba1 e c merge f merge f

Fig. 10. $Iba1^+$ cell infiltration in the SNpc after AAV/DJ-α-synuclein injection at 4 weeks. Representative fluorescence images of the injected- and non-injected SNpc 4 weeks after AAV/DJ-α-synuclein injection. TH^+ neurons (green) and $Iba1^+$ myeloid cells (white; "microglia") (a-f). Quantification of $Iba1^+$ associated changes in the SNpc (g, h). Infiltration of $Iba1^+$ cells in the injected SNpc can be observed (g, b-f). Additionally, the fluorescent intensity of $Iba1^+$ was increased at the injection site (h, b-f). Data shown: individual data points depict individual animals (contra- and ipsilateral side of each), paired values are connected by a line, box symbolizes the mean). All images were acquired with a 20 × magnification objective, scale bar: 100 μm.

transduction, AAV/DJ- α -synuclein, AAV/DJ-tdTomato, AAV/6- α -synuclein and AAV/6-tdTomato, respectively) can be seen in Fig. 1a-p and Fig. 2a-p.

There was successful viral transduction with both, the AAV/DJ and the AAV/6 serotype. Thus, to determine the most suitable AAV serotype for *in vivo* stereotaxic application, transduction efficiencies of both serotypes were assessed.

There was a significantly higher number of transduced DA cells that were treated with a viral construct of the AAV/DJ serotype (both α -synuclein or tdTomato 85 %) compared to the respective AAV/6 serotype (α -synuclein: 65 % or tdTomato: 63 %) (Fig. 3).

However, quantification of protein levels revealed no difference in transduction efficiencies of the viral constructs AAV/DJ- α -synuclein and AAV/6- α -synuclein (Suppl. Fig. 1a-b).

3.2. Evaluation of the AAV/DJ- α -synuclein viral construct in vivo

Thirty-four adult rats received a unilateral injection of AAV/DJ carrying the human <code>SNCA</code> into the right SNpc (1 $\times 10^{10}$ vg/µL). Twelve rats received a unilateral injection of AAV/DJ carrying red fluorescent tdTomato into the right SNpc (1 $\times 10^{10}$ vg/µL) and further 12 rats were sham (1 $\times PBS$) operated. Before <code>in vivo</code> injection, transduction efficiency

of the viral vectors was evaluated in DA progenitor cells *in vitro* as described to ensure overexpression of the viral inserts of the human SNCA encoding for α -synuclein (85 %) and the dTomato gene encoding for the tdTomato protein (85 %), respectively. Morphological and behavioral changes were examined 4, 8, 12 and 16 weeks post viral vector injection and compared to healthy stages (baseline behavioral measurement) retrieved prior to stereotaxic injection.

3.2.1. Degeneration of DA neurons in the injected SNpc and their corresponding fibers projecting to the ipsilateral STR at 4-, 8-, 12- and 16 weeks post AAV/DJ- α -synuclein injection

Based on the high transduction efficiency of the AAV/DJ- α -synuclein viral vector construct and its control vector AAV/DJ-tdTomato, we examined whether a progressive *in vivo* rat model could be established by the use of those particular vectors. First, histological hallmarks including the degeneration of DA neurons located in the SNpc and their fiber projections to the STR were determined. Exemplary staining of DA neurons either overexpressing the α -synuclein or the tdTomato protein are shown as co-localizations of TH⁺ and α -synuclein⁺ or tdTomato⁺, respectively (Fig. 4a-o).

Further, remaining DA neurons within the injected SNpc were quantified by stereological analysis in all animals (Fig. 5a and b). The

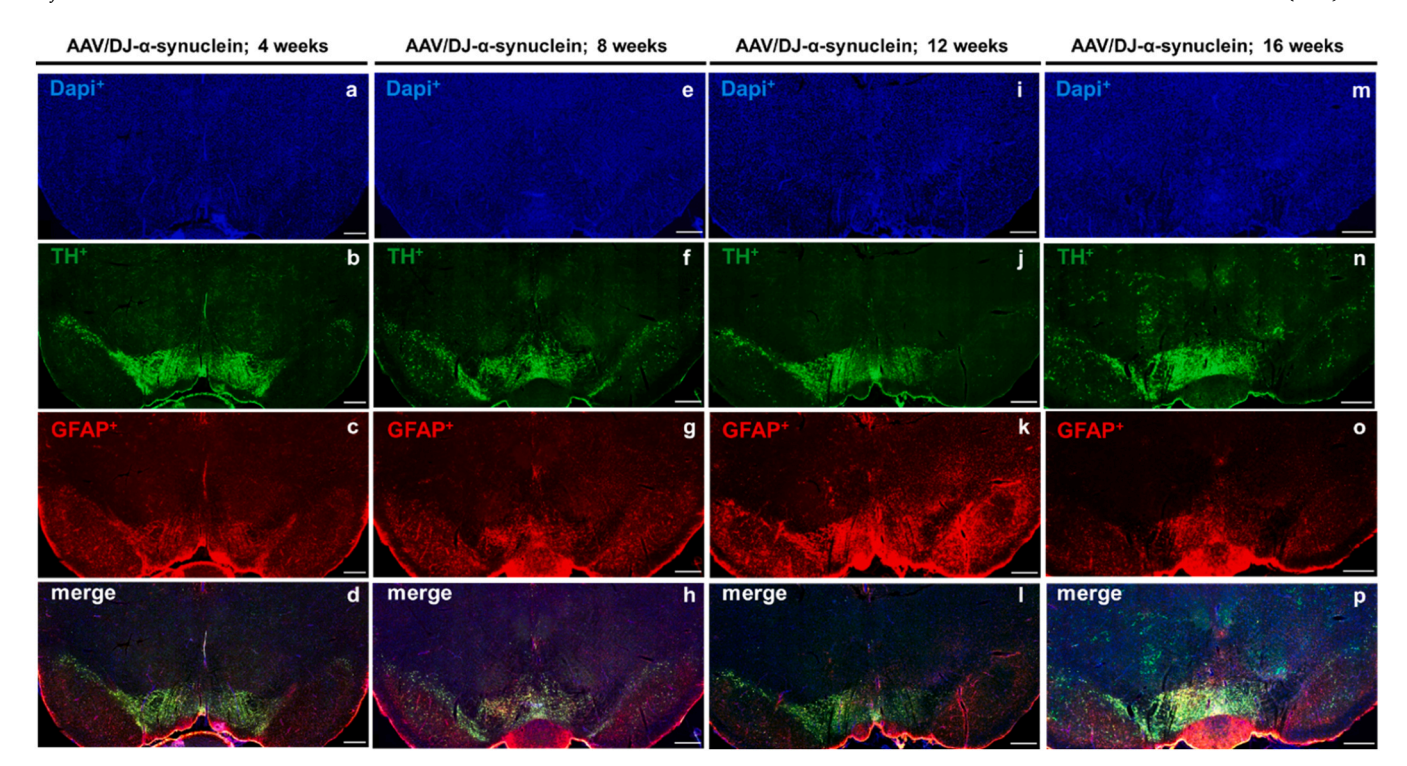


Fig. 11. GFAP⁺ cell infiltration in the SNpc after AAV/DJ- α -synuclein injection at 12 weeks. Representative fluorescence staining of nuclei (Dapi⁺), remaining TH⁺ neurons (green) and GFAP⁺ astrocytes (red) located in the SNpc after AAV/DJ- α -synuclein injection at 4 (a-d), 8 (e-h), 12 (i-l) and 16 weeks (m-p). All images were acquired with a 20 × magnification objective. Scale bar is 500 μm.

estimated number of DA neurons in the non-injected contralateral hemisphere was in accordance with earlier studies (Koprich et al., 2010; Nair-Roberts et al., 2008; von Hövel et al., 2019) and served as control.

Rats injected with AAV/DJ-α-synuclein showed a significant decrease of DA neurons within the injected SNpc after 8 (50.8 % remaining TH⁺ neurons; 3508 absolute remaining TH⁺ neurons), 12 (54.2 % remaining TH⁺ neurons; 3797 absolute remaining TH⁺ neurons) and 16 (49.1 % remaining TH⁺ neurons; 3044 absolute remaining TH⁺ neurons) weeks compared to rats injected with AAV/DJ-tdTomato or sham (1 ×PBS) operated animals, respectively. Although a tendency towards a decrease was also evident 4 weeks post injection (78.9 % remaining TH⁺ neurons), no statistical significance was evident. Contrary to the animals injected with AAV/DJ-α-synuclein, neither AAV/DJtdTomato (4 weeks: 97.3 %; 5837 absolute TH⁺ neurons, 8 weeks: 119.3 %; 5575 absolute remaining TH⁺ neurons, 12 weeks: 109.0 %; 6596 absolute remaining TH⁺ neurons and 16 weeks: 104.3 %; 6605 remaining TH⁺ neurons, respectively) nor sham operated rats (1 ×PBS; 4 weeks: 94.6 %; 5493 absolute remaining TH⁺ neurons, 8 weeks: 111.3 %; 7678 absolute remaining TH⁺ neurons, 12 weeks: 90.3.0 %; 6605 absolute remaining TH+ neurons and 16 weeks: 103.0 %; 6835 absolute remaining TH⁺ neurons remaining TH⁺ neurons, respectively) showed decreased DA neuron numbers over time.

Since loss of DA neurons in the SNpc is accompanied by loss of DA fibers innervating the related STR, the density of TH^+ fibers reaching the STR was evaluated at 6 different coronal levels (AP: +1.2; +0.96; +0.72; +0.48; +0.24 and 0.0 relative to bregma) (Paxinos and Watson, 2013). The healthy contralateral STR was used as a control (Fig. 6a-b).

In line with the results obtained from the stereological assessment of the remaining TH $^+$ neurons in the SNpc, animals injected with AAV/DJ- α -synuclein also showed a significant loss of remaining axonal fiber density in the ipsilateral STR after 4 (73.5 % remaining fiber density), 8 (57.2 % remaining fiber density), 12 (59.8 % remaining fiber density) and 16 (58.2 % remaining fiber density) weeks, respectively, compared to rats injected with AAV/DJ-tdTomato or sham (1 ×PBS) operated animals (Fig. 6c). Although a tendency towards a decrease was also

evident 4 weeks post injection (73.5 % remaining TH $^+$ fiber density), statistical significance was not reached. Contrary to the animals injected with AAV/DJ- α -synuclein, rats injected with either AAV/DJ-tdTomato (4 weeks: 91.4 %, 8 weeks: 94.6 %, 12 weeks: 84.8 % and 16 weeks: 93.7 % remaining fiber density, respectively) or sham operated rats (1 ×PBS; 4 weeks: 100.3 %, 8 weeks: 98.3 %, 12 weeks: 97.7 % and 16 weeks: 94.1 % remaining fiber density, respectively) did not show decreased DA neuron fiber density at any timepoint.

To further determine if the observed degeneration of DA neurons only affects a certain subtype of DA cells, we distinguished between $Girk^+$ A9 DA neurons located mainly in the SNpc and Calbindin⁺ A10 DA neurons mainly found in the ventral tegmental area (VTA) (Dahlstroem and Fuxe, 1964). First, we elucidated whether $Girk^+$ DA neurons are more prone to degenerate over time. This subset of DA neurons was found in most parts of the SNpc and to lesser extent in the VTA (Fig. 7a-d). While $Girk^+$ dopaminergic neurons appear qualitatively susceptible to AAV/DJ- α -synuclein-induced degeneration, a quantitative analysis would be necessary to clearly define the vulnerability profile of this specific neuronal subset. Nonetheless, $Girk^+$ DA neuronal degeneration overlaps with the detected degeneration of TH^+ DA neurons of the SNpc over time (Fig. 8d, h, l, p).

The subpopulation of Calbindin⁺ DA neurons was mainly found in the VTA and the lateral tier of the SNpc. Some Calbindin⁺ DA neurons were also visible in the dorsal tier of the SNpc, while the ventral part of the SNpc did not show any Calbindin⁺ DA neurons (Fig. 9a-d). Over time, no difference of Calbindin⁺ DA neurons was detected, showing that Calbindin⁺ DA neurons do not show any vulnerability towards AAV/DJ- α -synuclein induced degeneration (Fig. 8d, h, l, p).

3.2.2. Formation of insoluble α -synuclein inclusions in the AAV/DJ- α -synuclein injected hemisphere

The formation of insoluble fibrillary aggregates of human α -synuclein protein is one of the main hallmarks of PD. Staining against the S129-phosporylated α -synuclein after proteinase K treatment revealed that only rats injected with AAV/DJ- α -synuclein formed insoluble

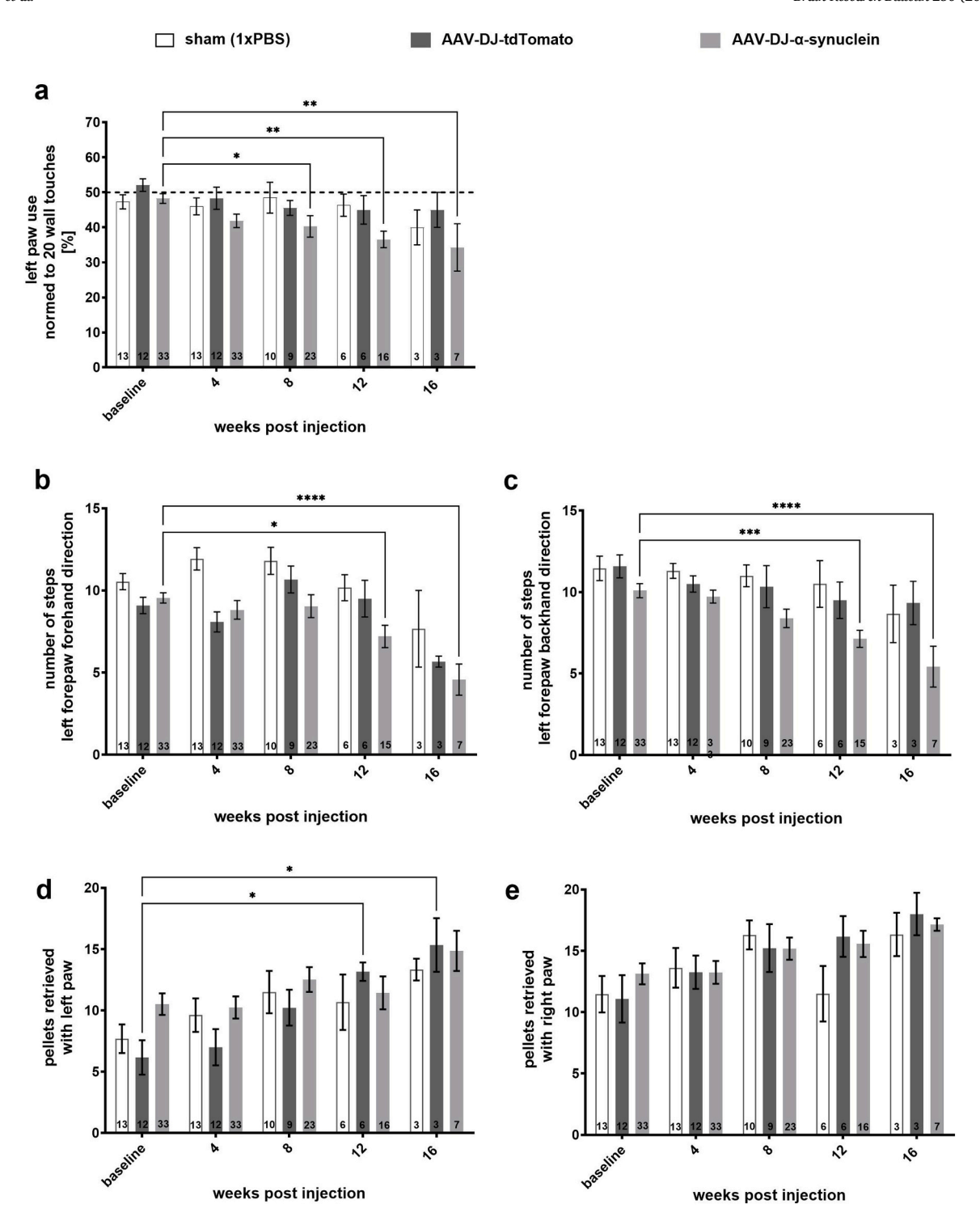


Fig. 12. Behavioral tests. Left forepaw use in the cylinder test as percentage of wall touches normed to 20 total wall touches at baseline, 4, 8, 12 and 16 weeks post (viral or 1 ×PBS) injection (a). Adjusting steps in the stepping test in the forehand (b) and backhand (c) direction of the left paw at baseline, 4, 8, 12 and 16 weeks post (viral or 1 ×PBS) injection. Number of pellets retrieved in the staircase test with the left (d) and right (e) paw at baseline, 4, 8, 12 and 16 weeks post (viral or 1 ×PBS) injection. Data are represented as mean \pm SEM (repeated measurements). Two-way ANOVA followed by Dunnett's post hoc analysis with *p < 0.5, **p < 0.01, ***p < 0.001 and ****p < 0.0001. Comparison of AAV/DJ-α-synuclein injected animals at 4 (n = 33), 8 (n = 23), 12 (n = 16) and 16 (n = 7) weeks to their individual baseline measurement (n = 33), respectively.

inclusions in the injected hemisphere compared to sham operated and AAV/DJ-tdTomato injected rats at 16 weeks post injection (Fig. 9a-i). Interestingly, these inclusions were not only visible in the SNpc and its surrounding areas but also in the cortex and the STR (data not shown).

3.2.3. Early signs of neuroinflammation in the AAV/DJ- α -synuclein injected hemisphere

Increased expression of the human α -synuclein protein by viral vector can lead to microglia accumulation and a decrease of a homeostatic microglia phenotype. In order to assess changes of myeloid cells, rat brain tissue was stained against Iba1, a marker of myeloid cells,

Comparative overview of AAV-Syn1 rat PD models adapted from (Huntington and Srinivasan, 2021).

Paper (Year)	Animal/ sex	Inj. age (wks)	Serotype Promoter	Promoter	α-syn strain	Enhancers Viral load (gc)	Viral load (gc)	Length of expression (wks)	TH loss SNpc	DA loss Str	Behavioral tests	Insoluble α -syn inclusions	Inflammatory response
Kefalakes et al.	SD Rats / F	16	rAAV/ DJ	Syn1	WT	I	1.0E+ 10	4, 8, 12, 16	21–51 %	26-42 %	Staircase Stepping	yes	Iba1, GFAP
Klein et al. (2002)	SD Rats/	12	AAV	CBA	A30P	1	1.0E+13	4-12	53 %	ı	Cyunder rotation	likely	1
Koprich et al. (2010)	SD Rats/ F	8-10	AAV1/2	CBA/ CMV	A53T	WPRE	5.1E+12	approx. 8–12	Ca. 51 %	significant	I	yes	I
Decressac et al. (2012)	SD Rats/ F	8–10	AAV6	$\begin{array}{c} Syn1 + WPRE/\\ CBA \end{array}$	WT	WPRE	3.7E+ 12 3.0E+ 12	Up to 16	> 50 %	> 50 %	Cylinder Rotation	yes	1
von Hövel et al. (2019)	SD Rats/ F	16	AAV2/ DJ	Syn1	WT / E46K	1	4.0E+ 08 4.3E+ 08	4, 8, 12	WT: 0 %	WT: 66 % E46K: 60 %	Cylinder, Rotation	yes	I
Østergaard et al. (2020)	SD Rats/ F	ca. 10–12	AAV2/5	CBA	WT	ı	30E + 10	up to 11	E46K: 34 % not quantified	not quantified	Cylinder VEP	yes	ı
Kelly et al. (2021)	SD Rats/ F	8-10	AAV6	PGK1	WT & A53T	I	1.67E + 10 1.33E + 10	4	none	1	Stepping Whisker	yes	ı
Negrini et al. (2022)	SD Rats/ F	Ca. 10–12	AAV6	Syn1	WT	1	4.7E+ 14	4, 16	significant	significant	Stepping Cylinder rotation	yes	Iba1

which includes microglia, CNS-associated macrophages and monocyte-derived cells that infiltrate the brain (Paolicelli et al., 2022). The ipsi-lateral SNpc of sham (1 ×PBS) operated animals and after AAV/DJ-tdTomato injection did not show increased numbers of Iba1 $^+$ cells (data not shown). A direct ipsi- to contralateral comparison of AAV/DJ- α -synuclein animals was chosen to identify direct intra-animal effects of AAV/DJ- α -synuclein injection at 4 weeks post injection (Fig. 10a-h). Following injection, a significant increase in Iba1 $^+$ cells was observed (Fig. 10g), combined with an increase of Iba1 $^+$ fluorescent intensity (Fig. 10h). This is indicative of microglia infiltration and/or clonal expansion in response to AAV/DJ-mediated α -synuclein overexpression.

Similar to microglia, astrocytes can be detected by the marker GFAP (Palfreyman et al., 1979). Astrocyte infiltration and expansion was evaluated at 4, 8, 12 and 16 weeks. Thereby, the ipsi- to contralateral qualitative comparison was chosen to identify direct intra-animal effects of an AAV/DJ- α -synuclein induced lesion at all examined timepoints (Fig. 11). Apart from this, both hemispheres were also compared in sham and AAV/DJ-tdTomato injected rats with no evident difference (data not shown). Following AAV/DJ- α -synuclein injection, a qualitative increase in GFAP⁺ cells was observed at 12 weeks post-injection, which appeared reduced by 16 weeks. These observations suggest a transient astrocytic response to AAV/DJ-mediated human α -synuclein overexpression, although further quantitative analyses would be necessary to confirm the extent and dynamics of astrocyte activation.

3.2.4. Progressive motor impairment of the left forepaw in both the cylinder and the stepping test

Since motor impairments of PD usually manifest themselves in a progressive manner in late adulthood, we aimed to measure disease progression by evaluating different timepoints (Hoehn and Yahr, 1967; Schwab, 1960). Therefore, behavioral alterations caused by unilateral α -synuclein overexpression were evaluated at baseline (before injection), 4-, 8-, 12- and 16 weeks post injection. Motor performance of all rats throughout the experimental period was evaluated in the cylinder, the stepping- and the staircase test.

Spontaneous forelimb asymmetry was assessed by use of the cylinder test (Schallert et al., 2000). Sham (1 × PBS) operated animals and animals receiving AAV/DJ-tdTomato did not show any alterations in motor behavior over time (Fig. 12a). Baseline sham: $47.3 \pm 1.9 \%$, 4 weeks: 46.0 ± 2.3 %, 8 weeks: 48.5 ± 4.2 %, 12 weeks: 46.3 ± 2.9 % and 16 weeks: 40.0 ± 4.1 % and baseline AAV/DJ-tdTomato: 52.1 ± 1.7 %, 4 weeks: $48.3 \pm 3.0 \%$, 8 weeks: $45.6 \pm 2.0 \%$, 12 weeks: $45.0 \pm 3.7 \%$ and 16 weeks: 45.0 \pm 4.1 %, respectively. Although both sham operated rats and AAV/DJ-tdTomato injected rats showed a tendency towards a decrease in forelimb use at 16 weeks post injection, this decrease can be caused by the low animal number (3 rats were used at 16 weeks for both the sham and the AAV/DJ-tdTomato group), also indicated by higher SEMs. Contrary, rats injected with AAV/DJ-α-synuclein showed a progressive deterioration of the left paw used to spontaneously touch the walls of the glass cylinder over time: baseline: 48.2 \pm 1.4 %, 4 weeks: 41.8 \pm 1.9 %, 8 weeks: 40.3 \pm 3.0 %, 12 weeks: 36.6 \pm 2.3 % and 16 weeks: 34.3 \pm 6.3 %, respectively. It reached statistical significance at 8, 12 and 16 weeks compared to baseline measurement. However, no statistic correlation was registered between the percentage left forepaw asymmetry in the cylinder test and the percentage of remaining TH+ cells in the injected SNpc or the remaining TH⁺ fibers in the ipsilateral STR (Suppl. Fig. 2a-f).

Forelimb akinesia was further evaluated in the stepping test (Olsson et al., 1995). Here, the left paw's forehand and backhand movement (number of adjusting steps) was assessed (Fig. 12b). Similar to the cylinder test, there were no differences observed in sham (1 ×PBS) operated animals or animals injected with AAV/DJ-tdTomato. Baseline sham: 10.5 ± 0.5 , 4 weeks: 11.9 ± 0.7 , 8 weeks: 11.8 ± 0.8 , 12 weeks: 10.2 ± 0.7 and 16 weeks: 10.9 ± 0.7 and baseline AAV/DJ-tdTomato: 10.9 ± 0.5 , 4 weeks: 10.9 ± 0.5 , 4 weeks: 10.9 ± 0.5 , 12 weeks: 10.9 ± 0.5 , 13 weeks: 10.9 ± 0.5 , 14 weeks: 10.9 ± 0.5 , 15 weeks: 10.9 ± 0.5 , 16 weeks: 10.9 ± 0.5 , 17 weeks: 10.9 ± 0.5 , 18 weeks: 10.9 ± 0.5 , 19 weeks: 1

 \pm 1.0 and 16 weeks: 5.7 \pm 0.3, respectively. Both sham operated rats and AAV/DJ-tdTomato injected rats showed a decrease in the number of steps performed in forehand direction with the left forepaw at 16 weeks post injection, which is in agreement with the results of the cylinder test. However, this decrease was not statistically significant due to a lower number of animals evaluated as indicated by higher SEMs. Rats injected with AAV/DJ-α-synuclein showed a progressive decrease in the number of performed steps with the left forepaw in the forehand direction: baseline: 9.5 \pm 0.3, 4 weeks: 8.8 \pm 0.6, 8 weeks: 9.0 \pm 0.7, 12 weeks: 7.2 \pm 0.6 and 16 weeks: 4.6 \pm 0.9, respectively. Statistical significance was reached at 12 and 16 weeks compared to baseline measurement. Similar results were retrieved for the performance of the left forepaw in the backhand direction as there were no differences observed in sham (1 ×PBS) operated animals or animals injected with AAV/DJ-tdTomato (Fig. 12c). Baseline sham: 11.5 ± 0.7 , 4 weeks: 11.3 ± 0.4 , 8 weeks: $11.0 \pm 0.6,\, 12$ weeks: 10.5 ± 1.3 and 16 weeks: 8.7 ± 1.4 and baseline AAV/DJ-tdTomato: 11.6 ± 0.7 , 4 weeks: 10.5 ± 0.5 , 8 weeks: 10.3 \pm 1.2, 12 weeks: 9.5 \pm 1.0 and 16 weeks: 9.3 \pm 1.1, respectively. Animals injected with AAV/DJ-α-synuclein stepped less with the left forepaw in the backhand direction: baseline: 10.1 ± 0.4 , 4 weeks: 9.7 ± 0.4 , 8 weeks: 8.4 ± 0.6 , 12 weeks: 7.1 ± 0.5 and 16 weeks: 5.4 ± 1.2 , respectively. Statistical significance was reached at 12 and 16 weeks compared to baseline measurement. No statistic correlation was registered between the number of adjusting steps of the left paw in the forehand direction in the stepping test and the percentage of remaining TH⁺ cells in the injected SNpc or the remaining TH⁺ fibers in the ipsilateral STR (Suppl. Fig. 3 and 4a-f).

Fine motor skills were assessed by use of the staircase test (Montoya et al., 1991). Both left and right forepaw fine motor skills (ability to reach, grasp and retract food pellets) were evaluated (Fig. 12d-e). Unlike the cylinder and the stepping test, animals injected with AAV/DJ-tdTomato showed a statistically significant increase in fine motor skills of the left forepaw at 12 and 16 weeks post injection although there were no differences in fine motor performance of the left forepaw in sham (1 ×PBS) and AAV/DJ- α -synuclein operated animals. Baseline sham: 7.7 ± 1.1 , 4 weeks: 9.6 ± 1.3 , 8 weeks: 11.5 ± 1.6 , 12 weeks: 10.7 ± 2.1 and 16 weeks: 13.3 ± 0.7 and baseline AAV/DJ- α -synuclein: 10.5 ± 0.9 , 4 weeks: 10.2 ± 0.9 , 8 weeks: 12.5 \pm 1.0, 12 weeks: 11.4 \pm 1.3 and 16 weeks: 14.9 \pm 1.5, respectively. Baseline AAV/DJ-tdTomato: 6.2 ± 1.3 , 4 weeks: 7.0 ± 1.4 , 8 weeks: 10.2 ± 1.4 , 12 weeks: 13.2 ± 0.7 and 16 weeks: 15.3 ± 1.8 , respectively. Although there was a tendency towards an increase in fine motor skills of the right forepaw, no statistical differences were detected in neither of the groups. Baseline sham: 11.5 \pm 1.4, 4 weeks: 13.6 \pm 1.6, 8 weeks: 16.3 \pm 1.1, 12 weeks: 11.5 \pm 2.1 and 16 weeks: 16.3 \pm 1.4 and baseline AAV/DJ-tdTomato: 11.1 \pm 1.8, 4 weeks: 13.3 \pm 1.3, 8 weeks: $15.2 \pm 1.8, \ 12$ weeks: 16.2 ± 1.5 and 16 weeks: $18.0 \pm 1.4, \ respec$ tively. AAV/DJ- α -synuclein baseline: 13.1 \pm 0.8, 4 weeks: 13.2 \pm 0.9, 8 weeks: 15.2 ± 0.9 , 12 weeks: 15.6 ± 1.0 and 16 weeks: 17.1 ± 0.5 , respectively. All mean values registered in the right forepaw showed higher mean values compared to the respective mean values of the left forepaw pointing towards a right forepaw handedness of the animals tested. Due to the improvement of skilled motor performance, statistic correlation was not measured in the staircase test.

4. Discussion

A wide range of AAV-based animal models have been developed to investigate PD pathology through targeted overexpression of $\alpha\text{-synuclein}$ (Table 1). Within this landscape, our study introduces a particularly methodologically refined model system which provides (i) a neuroinflammatory component at an early disease state indicating that neuroinflammation goes with neurodegeneration and reflecting the situation in PD patients and, (ii) a comprehensive and multidimensional behavioral testing strategy to cover a broader spectrum of PD-related

motor deficits which potentially allows detection of smaller yet relevant treatment effects in future translational studies using this model, (iii) a moderate viral dose which strikes a deliberate balance between achieving consistent α -synuclein pathology and avoiding artifacts associated with supraphysiological transduction levels. This was achieved using the AAV-DJ serotype - a synthetic capsid variant that merges the transduction efficiencies of several conventional serotypes. This vector enables robust and efficient gene delivery to dopaminergic neurons, offering a clear advantage over more commonly used serotypes such as AAV2, AAV6, or AAV1/2. Coupled with the neuron-specific synapsin 1 promoter, our system achieves selective and physiologically relevant overexpression of α -synuclein, compared to the broader and often less targeted expression driven by ubiquitous promoters like CBA or CMV.

Spreading of α -synuclein is a core hallmark of PD, as α -synuclein containing LB-like inclusions can expand from patient tissue to exogenously administered healthy cell grafts (Kordower et al., 2008). So far, state of the art models include transgenic mouse models overexpressing α -synuclein, the injection of α -synuclein containing fibrils or viral-mediated models based on AAVs or lentiviruses (Simons and Fleming, 2023). AAVs are the most commonly used viruses due to their high ability to transduce neurons, their small size, which allows an easy expansion within the host tissue and their minimal immunogenic reaction. Also, AAVs rarely integrate into the hosts' genome increasing their working safety, thus, showing higher applicability than lentiviruses (Gómez-Benito et al., 2020; Konnova and Swanberg, 2018). To ensure neuron transduction, the human synapsin 1 promoter was applied (Kügler et al., 2003; Van der Perren et al., 2011). Although a promoter exclusively targeting dopaminergic (DA) neurons has not yet been employed in α -synuclein overexpression models, there are approaches utilizing Cre-dependent AAV systems in transgenic rats and mice expressing Cre recombinase systems for cell-specific expressions (Liu et al., 2016; Grames et al., 2018; Garcia Moreno et al., 2024). However, these studies have generally reported limited effects on DA neuron viability and, in one case, observed hyperlocomotion, raising questions about the robustness and translational relevance of such models.

We found that AAV/DJ showed one of the highest transduction efficiencies in vitro. In vivo AAV/DJ-mediated overexpression of the human α -synuclein protein resulted in a significant loss of DA neurons in the injected SNpc. Accordingly, striatal fiber density also decreased as DA neurons lose their innervation terminals in the STR leading to striatal denervation (Musacchio et al., 2022). Earlier studies demonstrated that this process strongly depends on viral titers, the α -synuclein insert itself (mutated or not) and α-synuclein oligomer- or fibril formation (Conway et al., 2000; Oliveras-Salvá et al., 2013; Winner et al., 2011). Fibrillar α -synuclein aggregates disrupt the endogenous expression of α -synuclein and lead to a pathological spread throughout the nervous system (Volpicelli-Daley et al., 2011). Although appearance and spreading of Lewy pathology is known to follow Braak's staging, recently an additional subtype showing a body-first spreading has emerged (Horsager et al., 2020). We further found that proteinase K resistant inclusions of phosphorylated α -synuclein were visible. The presence of α -synuclein aggregates correlates with the appearance of motor, psychiatric and cognitive symptoms (Beach et al., 2009). In our study, Lewy pathology coincides with the appearance of motor symptoms in the cylinder and the stepping test as well as the degeneration of DA neurons of the SNpc and their fibers reaching the STR.

Midbrain DA neurons are located in the retrorubral field, the SNpc and the VTA (Carlsson et al., 1962; Dahlstroem and Fuxe, 1964). The SNpc can be divided into a medial, dorsal, lateral and ventral tier consisting of DA clusters (Reyes et al., 2012). DA neurons show a heterogeneous vulnerability, with the ventral tier being much more vulnerable than the dorsal tier towards α -synuclein-induced toxicity (Damier et al., 1999; Gibb and Lees, 1991). Although this vulnerability has not been linked to molecular differences of DA subtypes yet, a categorization based on immunohistologic markers is possible (Dopeso-Reyes et al., 2014; Poulin et al., 2014; Thompson et al., 2005). DA neurons of the

SNpc can be predominantly identified by a higher Girk2 expression, whereas DA neurons located in the VTA mainly, but not exclusively, express Calbindin (Chung et al., 2005; Dahlstroem and Fuxe, 1964; Dopeso-Reyes et al., 2014; Thompson et al., 2005). These findings are in line with our results since we detected Girk⁺ neurons in all areas of the SNpc and only some in the VTA. Studies using double-labeled immunohistochemistry have shown that most TH⁺ neurons in the SNpc do not express Calbindin, while many Calbindin⁺ neurons in the adjacent SN pars lateralis or VTA do not express TH (Nemoto et al., 1999, Liang et al., 1996). This lack of colocalization is often used to distinguish vulnerable TH⁺ (in terms of PD) neurons from resistant populations (Dopeso-Reyes et al., 2014). We found Calbindin⁺ neurons to be predominantly located in the VTA and the lateral tier of the SNpc. Noticeably, Calbindin+ neurons were less prone to degenerate. Calbindin is a calcium-binding protein involved in the buffering of intracellular calcium, therefore Calbindin⁺ neurons are resistant to PD-associated neurodegeneration, probably due to their better calcium buffering capacity (Inoue et al., 2019). Contrary, Girk⁺ neurons were highly affected concomitant to the degeneration of TH⁺ neurons of the SNpc.

Glial cells, especially microglia and astrocytes, impact PD initiation and progression (Halliday and Stevens, 2011). While neuroinflammatory responses exist to clear cellular debris and pathogens, they can also promote neurodegeneration when overly active. Activated microglia is identified by common macrophage markers including Iba1 (Ito et al., 1998). We found an increased Iba⁺ microglia density in the SN of AAV/DJ-α-synuclein injected rats. In line with our results, microglia activation is described in early PD stages prior to DA degeneration of the SN (He et al., 2002; Sherer et al., 2003; Su et al., 2009). Moreover, there is strong evidence that microglia become activated and enriched as a reaction to α-synuclein accumulating, thus, enhancing α-synuclein-related pathology and DA cell loss (Zhang et al., 2005; Zheng and Zhang, 2021). Besides accumulating altered α-synuclein, astrocytes propagate neurodegeneration via exacerbating microglia activation by release of inflammatory stimuli within the microglia-astrocyte crosstalk (Sun et al., 2016). Our findings show first qualitative cues of GFAP⁺ astrocyte clustering around the SNpc post AAV/DJ-α-synuclein injection. At 16 weeks post injection, this effect is diminished supporting the fact that extensive α -synuclein accumulation suppresses astrocyte activation at exacerbated disease end stages (Tong et al., 2015). Altogether, glia propagates early α-synuclein-dependent neuroinflammation within our model, as the inflammatory responses detected were neither AAV-induced nor associated with the surgical procedure itself. Although PD is not an autoimmune disease, neuroinflammation is prominent in PD patients with some inflammatory responses preceding motor phenotypes (Lindestam Arlehamn et al., 2020).

Apart from the histological hallmarks of PD, one of the most crucial aspects is the development of motor impairment. In animal models of PD, motor deficits typically begin when 40–50 % of dopamine (DA) neurons are lost, with 60–70 % of their nerve fibers still able to reach the striatum (STR) (Decressac et al., 2012; Gombash et al., 2013; Kirik et al., 2002). In our model, the severity of motor deficits directly corresponds to the extent of DA neuron loss and the progression of the disease.

The cylinder test is widely used to assess forelimb use asymmetry after a unilateral lesion of the SNpc (Decressac et al., 2012; Schallert et al., 2000; von Hövel et al., 2019). Rats injected with AAV/DJ-α-synuclein developed a forelimb use asymmetry. This decrease was registered by an increased voluntary use of the right forepaw (ipsilateral to lesion site). Taken together, the detected left forepaw use asymmetry (contralateral to lesion site) is comparable to studies reporting significant impairment in correlation with a 45 % neuron loss in the SNpc and/or their projecting fibers to the STR (Decressac et al., 2012). Here, the handedness of the animals, needs to be considered as it is independent of the learning process during the execution of a motor task (Miklyaeva et al., 1991). Specifically, Sprague-Dawley rats are described to show a right-pawed handedness regardless of sex (Pence, 2002). Similarly, rats injected with

AAV/DJ- α -synuclein developed a decrease in the number of adjusting steps in both the forehand and backhand direction in the stepping test. The stepping test assesses deficits in forelimb stepping in the contralateral side of the lesion (Cederfjäll et al., 2012; Olsson et al., 1995). Sham- and AAV/DJ-tdTomato injected animals showed fluctuations in both the forehand and backhand direction. This variation can be explained by the lower number of animals used within these groups as well as the higher susceptibility of the stepping test due to the direct interaction of the animal with the experimenter (Olsson et al., 1995).

Contrary, a general increase in fine motor skills was observed in the staircase test. Surprisingly, rats injected with a AAV/DJ-tdTomato showed an improvement in the contralateral side of the lesion (left forepaw). The staircase test assesses skilled forepaw use as it combines distinct forepaw movements (reach, grasp and retract) including a rotatory movement, which renders it the most sensitive test of our study (Klein and Dunnett, 2012; Montoya et al., 1991; Nica et al., 2017; Whishaw et al., 2008, 1997). Although it is a consistent test to evaluate motor impairment, acclimatization and training need to be sufficient (Cederfjäll et al., 2012; Nikkhah et al., 1998). Within this study, a training of two weeks was applied during which acclimatization time in the box was steadily increased before baseline measurement. The measured increase in performance shows that a performance plateau was not reached yet. Thus, a longer training would have been necessary. Although the training and acclimatization phase was chosen according to stable performance phases of previous works, evaluation periods vary (Stößel et al., 2017; Whishaw et al., 1997). Nonetheless, strain-dependencies in performance renders the comparison to other studies challenging (Nikkhah et al., 1998; Unis et al., 1991).

Our results provide strong evidence that the novel AAV/DJ viral construct, which overexpresses the human $\alpha\text{-synuclein}$ protein, effectively generates a rat model of PD. This model exhibits the key histopathological features of PD and develops a progressive motor impairment, making it a promising tool for testing future therapeutic strategies.

CRediT authorship contribution statement

Diana Peristich: Validation, Investigation, Data curation. Ekaterini Kefalakes: Writing – review & editing, Writing – original draft, Visualization, Validation, Supervision, Project administration, Methodology, Investigation, Formal analysis, Data curation. Franziska Mewes: Writing – review & editing, Visualization, Validation, Investigation, Data curation. Christopher Käufer: Writing – review & editing, Visualization, Validation, Investigation, Data curation. Regina Rumpel: Writing – review & editing, Supervision, Project administration, Methodology, Conceptualization. Julia Schipke: Visualization, Data curation. Friederike Schneider: Writing – review & editing, Supervision. Clara Plötner: Validation, Investigation, Data curation. Volodymyr Shcherbatyy: Validation, Data curation.

Funding information

This work was financially supported by Niedersächsisches Ministerium für Wissenschaft und Kunst: REBIRTH Innovation-/Synergy Grants of the Hannover Medical School-Forschungszentrum für translationale regenerative Medizin; Volkswagenstiftung (Niedersächsisches Vorab) ZN3440.

Declaration of Competing Interest

The authors declare that they have no conflict of interest. Parts of the results are encompassed in Franziska Mewes' doctoral thesis as well as in Diana Peristichs' and Clara Plötners' bachelor theses.

Acknowledgments

We thank Natascha Heidrich and Silke Fischer for their tremendous technical assistance regarding the immunohistochemistry of the brain slices. Moreover, we thank Jennifer Metzen for her assistance with the behavioral tests. Since we were unable to reach Maike Wesemann, we want to thank her for her technical support regarding the in vitro experiments.

Appendix A. Supporting information

Supplementary data associated with this article can be found in the online version at doi:10.1016/j.brainresbull.2025.111464.

Data Availability

Data will be made available on request.

References

- Azeredo da Silveira, S., Schneider, B.L., Cifuentes-Diaz, C., Sage, D., Abbas-Terki, T., Iwatsubo, T., Unser, M., Aebischer, P., 2009. Phosphorylation does not prompt, nor prevent, the formation of alpha-synuclein toxic species in a rat model of Parkinson's disease. Hum. Mol. Genet 18, 872-887.
- Barbeau, A., Murphy, G.F., Sourkes, T.L., 1961. Excretion of dopamine in diseases of basal ganglia. Science 133, 1706-1707.
- Beach, T.G., Adler, C.H., Lue, L., Sue, L.I., Bachalakuri, J., Henry-Watson, J., Sasse, J., Boyer, S., Shirohi, S., Brooks, R., Eschbacher, J., White, C.L., Akiyama, H., Caviness, J., Shill, H.A., Connor, D.J., Sabbagh, M.N., Walker, D.G., 2009. Unified staging system for Lewy body disorders: correlation with nigrostriatal degeneration, cognitive impairment and motor dysfunction. Acta Neuropathol. 117, 613-634.
- Ben Gedalya, T., Loeb, V., Israeli, E., Altschuler, Y., Selkoe, D.J., Sharon, R., 2009. Alphasynuclein and polyunsaturated fatty acids promote clathrin-mediated endocytosis and synaptic vesicle recycling. Traffic 10, 218-234.
- Benabid, A.L., Pollak, P., Seigneuret, E., Hoffmann, D., Gay, E., Perret, J., 1993. Chronic VIM thalamic stimulation in Parkinson's disease, essential tremor and extrapyramidal dyskinesias. Acta Neurochir. Suppl. (Wien.) 58, 39-44.
- Björklund, A., Stenevi, U., Schmidt, R.H., Dunnett, S.B., Gage, F.H., 1983. Intracerebral grafting of neuronal cell suspensions. I. Introduction and general methods of preparation. Acta Physiol. Scand. Suppl. 522, 1–7.
- Braak, H., Del Tredici, K., Rüb, U., de Vos, R.A., Jansen Steur, E.N.H., Braak, E., 2003. Staging of brain pathology related to sporadic Parkinson's disease. Neurobiol. Aging 24, 197-211.
- Burré, J., Sharma, M., Tsetsenis, T., Buchman, V., Etherton, M.R., Südhof, T.C., 2010. Alpha-synuclein promotes SNARE-complex assembly in vivo and in vitro. Science 329, 1663-1667,
- Carlsson, A., Falck, B., Hillarp, N.A., 1962. Cellular localization of brain monoamines. Acta Physiol. Scand. Suppl. 56, 1-28.
- Cederfjäll, E., Sahin, G., Kirik, D., Björklund, T., 2012. Design of a single AAV vector for coexpression of TH and GCH1 to establish continuous DOPA synthesis in a rat model of Parkinson's disease. Mol. Ther. 20, 1315-1326.
- Chung, C.Y., Seo, H., Sonntag, K.C., Brooks, A., Lin, L., Isacson, O., 2005. Cell typespecific gene expression of midbrain dopaminergic neurons reveals molecules involved in their vulnerability and protection. Hum. Mol. Genet 14, 1709-1725.
- Conway, K.A., Lee, S.J., Rochet, J.C., Ding, T.T., Williamson, R.E., Lansbury Jr Pt, 2000. Acceleration of oligomerization, not fibrillization, is a shared property of both alphasynuclein mutations linked to early-onset Parkinson's disease: implications for pathogenesis and therapy. Proc. Natl. Acad. Sci. USA 97, 571-576.
- Cotzias, G.C., Tang, L.C., Ginos, J.Z., 1974. Monoamine oxidase and cerebral uptake of dopaminergic drugs. Proc. Natl. Acad. Sci. USA 71, 2715-2719.
- Dahlstroem, A., Fuxe, K., 1964. Evidence for the existence of monoamine-containing neurons in the central nervous system. I. Demonstration of monoamines in the cell bodies of brain stem neurons. Acta Physiol. Scand. Suppl. 232, 1-55 (Suppl).
- Damier, P., Hirsch, E.C., Agid, Y., Graybiel, A.M., 1999. The substantia nigra of the human brain. I. Nigrosomes and the nigral matrix, a compartmental organization based on calbindin D(28K) immunohistochemistry. Brain 122 (Pt 8), 1421-1436.
- de Rijk, M.C., Launer, L.J., Berger, K., Breteler, M.M., Dartigues, J.F., Baldereschi, M., Fratiglioni, L., Lobo, A., Martinez-Lage, J., Trenkwalder, C., Hofman, A., 2000. Prevalence of Parkinson's disease in Europe: a collaborative study of populationbased cohorts. Neurologic Diseases in the Elderly Research Group. Neurology 54, S21-S23.
- Decressac, M., Mattsson, B., Lundblad, M., Weikop, M., Björklund, A., 2012. Progressive neurodegenerative and behavioural changes induced by AAV-mediated overexpression of α -synuclein in midbrain dopamine neurons. Neurobiol. Dis. 45,
- Dopeso-Reyes, I.G., Rico, A.J., Roda, E., Sierra, S., Pignataro, D., Lanz, M., Sucunza, D., Chang-Azancot, L., Lanciego, J.L., 2014. Calbindin content and differential vulnerability of midbrain efferent dopaminergic neurons in macaques. Front Neuroanat. 8, 146.

- Dorsey, E.R., Sherer, T., Okun, M.S., Bloem, B.R., 2018. The emerging evidence of the parkinson pandemic. J. Park. Dis. 8 (s1), S3-S8.
- Ehringer, H., Hornykiewicz, O., Lechner, K., 1961. The effect of methylene blue on monoamine oxidase and the catechol amine and 5-hydroxytryptamine metabolism of the brain. Naunyn. Schmiedebergs Arch. Exp. Pathol. Pharmakol. 241, 568-582.
- Fearnley, J.M., Lees, A.J., 1991. Ageing and Parkinson's disease: substantia nigra regional selectivity. Brain 114 (Pt 5), 2283-2301.
- Garcia Moreno, S.I., Limani, F., Ludwig, I., Gilbert, C., Pifl, C., Hnasko, T.S., Steinkellner, T., 2024. Viral overexpression of human alpha-synuclein in mouse substantia nigra dopamine neurons results in hyperdopaminergia but no neurodegeneration. Exp. Neurol. 382, 114959.
- GBD 2016 Parkinson's Disease Collaborators. Global, regional, and national burden of Parkinson's disease, 1990-2016: a systematic analysis for the Global Burden of Disease Study 2016 [published correction appears in Lancet Neurol. 2021 Dec;20 (12):e7. Lancet Neurol. 2018;17(11):939-953. https://doi.org/10.1016/s1474-(18)30295-3.
- Gibb, W.R., Lees, A.J., 1988. The relevance of the Lewy body to the pathogenesis of idiopathic Parkinson's disease. J. Neurol. Neurosurg. Psychiatry 51, 745-752.
- Gibb, W.R., Lees, A.J., 1991. Anatomy, pigmentation, ventral and dorsal subpopulations of the substantia nigra, and differential cell death in Parkinson's disease. J. Neurol. Neurosurg. Psychiatry 54, 388-396.
- Goetz, C.G., 2011. The history of Parkinson's disease: early clinical descriptions and neurological therapies. Cold Spring Harb. Perspect. Med 1, a008862.
- Gombash, S.E., Manfredsson, F.P., Kemp, C.J., Kuhn, N.C., Fleming, S.M., Egan, A.E., Grant, L.M., Ciucci, M.R., MacKeigan, J.P., Sortwell, C.E., 2013. Morphological and behavioral impact of AAV2/5-mediated overexpression of human wildtype alphasynuclein in the rat nigrostriatal system. PLoS One 8, e81426.
- Gómez-Benito, M., Granado, N., García-Sanz, P., Michel, A., Dumoulin, M., Moratalla, R., 2020. Modeling Parkinson's disease with the alpha-synuclein protein. Front Pharm. 11, 356.
- Grames, M.S., Dayton, R.D., Jackson, K.L., Richard, A.D., Lu, X., Klein, R.L., 2018. Credependent AAV vectors for highly targeted expression of disease-related proteins and neurodegeneration in the substantia nigra. FASEB J. 32 (8), 4420-4427.
- Grover, S., Kumar Sreelatha, A.A., Pihlstrom, L., Domenighetti, C., Schulte, C., Sugier, P. E., Radivojkov-Blagojevic, M., Lichtner, P., Mohamed, O., Portugal, B., Landoulsi, Z., May, P., Bobbili, D., Edsall, C., Bartusch, F., Hanussek, M., Krüger, J., Hernandez, D. G., Blauwendraat, C., Mellick, G.D., Zimprich, A., Pirker, W., Tan, M., Rogaeva, E., Lang, A., Koks, S., Taba, P., Lesage, S., Brice, A., Corvol, J.C., Chartier-Harlin, M.C., Mutez, E., Brockmann, K., Deutschländer, A.B., Hadjigeorgiou, G.M., Dardiotis, E., Stefanis, L., Simitsi, A.M., Valente, E.M., Petrucci, S., Straniero, L., Zecchinelli, A., Pezzoli, G., Brighina, L., Ferrarese, C., Annesi, G., Quattrone, A., Gagliardi, M., Burbulla, L.F., Matsuo, H., Kawamura, Y., Hattori, N., Nishioka, K., Chung, S.U., Kim, Y.J., Pavelka, L., van de Warrenburg, B.P.C., Bloem, B.R., Singleton, A.B., Aasly, J., Toft, M., Correia Guedes, L., Ferreira, J.J., Bardien, S., Carr, J., Tolosa, E., Ezquerra, M., Pastor, P., Diez-Fairen, M., Wirdefeldt, K., Pedersen, N.L., Ran, C., Belin, A.C., Puschmann, A., Hellberg, C., Clarke, C.E., Morrison, K.E., Krainc, D., Farrer, M.J., Kruger, R., Elbaz, A., Gasser, T., Sharma, M., 2022. Genome-wide association and meta-analysis of age at onset in parkinson disease: evidence from the COURAGE-PD consortium. Neurology 99, e698–e710. Halliday, G.M., Stevens, C.H., 2011. Glia: initiators and progressors of pathology in
- Parkinson's disease. Mov. Disord. 26, 6-17.
- He, Y., Le, W.D., Appel, S.H., 2002. Role of Fcgamma receptors in nigral cell injury induced by Parkinson disease immunoglobulin injection into mouse substantia nigra. Exp. Neurol. 176, 322-327.
- Hernandez, D.G., Reed, X., Singleton, A.B., 2016. Genetics in Parkinson disease: mendelian versus non-mendelian inheritance. J. Neurochem. 139 (1(1), 59-74.
- Hoehn, M.M., Yahr, M.D., 1967. Parkinsonism: onset, progression and mortality. Neurology 17, 427-442.
- Horsager, J., Andersen, K.B., Knudsen, K., Skjærbæk, C., Fedorova, T.D., Okkels, N., Schaeffer, E., Bonkat, Sk, Geday, J., Otto, M., Sommerauer, M., Danielsen, E.H., Becj, E., Kraft, J., Munk, O.L., Hansen, S.D., Pavese, N., Göder, R., Brooks, D.J., Berg, D., Borghammer, P., 2020. Brain-first versus body-first Parkinson's disease: a multimodal imaging case-control study. Brain 143, 3077–3088.
- Huntington, T.E., Srinivasan, R., 2021. Adeno-associated virus expression of α-synuclein as a tool to model Parkinson's disease: current understanding and knowledge gaps. Aging Dis. 12 (4), 1120-1137.
- Inoue, K.I., Miyachi, S., Nishi, K., Okado, H., Nagai, Y., Minamimoto, T., Nambu, A., Takada, M., 2019. Recruitment of calbindin into nigral dopamine neurons protects against MTP-induced parkinsonism. Mov. Disord. 34 (2), 200-209.
- Ito, D., Imai, Y., Ohsawa, K., Nakajima, K., Fukuuchi, Y., Kohsaka, S., 1998. Microgliaspecific localisation of a novel calcium binding protein, Iba1. Brain Res. Mol. Brain Res. 57, 1-9.
- Jia, F., Fellner, A., Kumar, K.R., 2022. Monogenic Parkinson's disease: genotype, phenotype, pathophysiology, and genetic testing. Genes (Basel) 13 (3), 471. Published 2022 Mar 7.
- Kelly, R., Cairns, A.G., Ådén, J., Almqvist, F., Bemelmans, A.P., Brouillet, E., Patton, T., McKernan, D.P., Dowd, E., 2021. The small molecule alpha-synuclein aggregator, FN075, enhances alpha-synuclein pathology in subclinical AAV rat models. Biomolecules 11 (11).
- Kirik, D., Rosenblad, C., Burger, C., Lundberg, C., Johansen, T.E., Muzyczka, N., Mandel, R.J., Björklund, A., 2002. Parkinson-like neurodegeneration induced by targeted overexpression of alpha-synuclein in the nigrostriatal system. J. Neurosci. 22, 2780-2791.
- Klein, A., Dunnett, S.B., 2012. Analysis of skilled forelimb movement in rats: the single pellet reaching test and staircase test. Curr. Protoc. Neurosci. Chapter 8 Unit8. 28.

- Klein, R.L., King, M.A., Hamby, M.E., Meyer, E.M., 2002. Dopaminergic cell loss induced by human A30P alpha-synuclein gene transfer to the rat substantia nigra. Hum. Gene. Ther. 13, 605-612.
- Konnova, E.A., Swanberg, M., 2018. Animal models of Parkinson's disease. In: Stoker, T. B., Greenland, J.C. (Eds.), Parkinson's Disease: Pathogenesis and Clinical Aspects. Codon Publications: Chapter 5.
- Koprich, J.B., Johnston, T.H., Reyes, M.G., Sun, X., Brotchie, J.M., 2010. Expression of human A53T alpha-synuclein in the rat substantia nigra using a novel AAV1/2 vector produces a rapidly evolving pathology with protein aggregation, dystrophic neurite architecture and nigrostriatal degeneration with potential to model the pathology of Parkinson's disease. Mol. Neurodegener. 5, 43.
- Kordower, J.H., Chu, Y., Hauser, R.A., Freeman, T.B., Olanow, C.W., 2008. Lewy bodylike pathology in long-term embryonic nigral transplants in Parkinson's disease. Nat. Med 14 (5), 504–506.
- Kügler, S., Kilic, E., Bähr, M., 2003. Human synapsin 1 gene promoter confers highly neuron-specific long-term transgene expression from an adenoviral vector in the adult rat brain depending on the transduced area. Gene Ther. 10, 337-347.
- Liang, C.L., Sinton, C.M., German, D.C., 1996. Midbrain dopaminergic neuronsin the mouse co-localization with Calbindin-D28K and calretinin, Neuroscience 75 (2),
- Lindestam Arlehamn, C.S., Dhanwani, R., Pham, J., Kuan, R., Frazier, A., Rezende Dutra, J., Phillips, E., Mallal, S., Roederer, M., Marder, K.S., Amara, A.W., Standaert, D.G., Goldman, J.G., Litvan, I., Peters, B., Sulzer, D., Sette, A., 2020. α-Synuclein-specific T cell reactivity is associated with preclinical and early Parkinson's disease. Nat. Commun. 11, 1875.
- Liu, Z., Brown, A., Fisher, D., Wu, Y., Warren, J., Cui, X., 2016. Tissue specific expression of cre in rat tyrosine hydroxylase and dopamine active transporter-positive neurons. PLoS One 11, e0149379.
- Lloyd, K.G., Davidson, L., Hornykiewicz, O., 1975. The neurochemistry of Parkinson's disease: effect of L-dopa therapy. J. Pharm. Exp. Ther. 195, 453-464.
- Lloyd, K., Hornykiewicz, O., 1970. Parkinson's disease: activity of L-dopa decarboxylase in discrete brain regions. Science 170, 1212-1213.
- Maroteaux, L., Campanelli, J.T., Scheller, R.H., 1988. Synuclein: a neuron-specific protein localized to the nucleus and presynaptic nerve terminal, J. Neurosci, 8, 2804–2815.
- Marsden, C.D., 1990. Parkinson's disease. Lancet 335, 948-952.
- McCown, T.J., 2005, Adeno-associated virus (AAV) vectors in the CNS, Curr, Gene Ther, 5. 333-338.
- Miklyaeva, E.I., Ioffe, M.E., Kulikov, M.A., 1991. Innate versus learned factors determining limb preference in the rat. Behav. Brain Res. 46, 103–115.
- Montoya, C.P., Campbell-Hope, L.J., Pemberton, K.D., Dunnett, S.B., 1991. The "staircase test": a measure of independent forelimb reaching and grasping abilities in rats. J. Neurosci. Methods 36, 219-228.
- Musacchio, T., Yin, J., Kremer, F., Koprich, J.B., Brotchie, J.M., Volkmann, J., Ip, C.W., 2022. Temporal, spatial and molecular pattern of dopaminergic neurodegeneration in the AAV-A53T α -synuclein rat model of Parkinson's disease. Behav. Brain Res. 432, 113968, 113968.
- Nair-Roberts, R.G., Chatelain-Badie, S.D., Benson, E., White-Cooper, H., Bolam, J.P., Ungless, M.A., 2008. Stereological estimates of dopaminergic, GABAergic and glutamatergic neurons in the ventral tegmental area, substantia nigra and retrorubral field in the rat. Neuroscience 152, 1024–1031.
- Negrini, M, Tomasello, G., Davidsson, M, et al., 2022. Sequential or Simultaneous Injection of Preformed Fibrils and AAV Overexpression of Alpha-Synuclein Are Equipotent in Producing Relevant Pathology and Behavioral Deficits. J. Parkinsons Dis. 12 (4), 1133-1153. https://doi.org/10.3233/JPD-212555.
- Nemoto, C., Hida, T., Arai, R., 1999. Calretinin and calbindin-D28k in dopaminergic neurons of the rat midbrain: a triple-labeling immunohistochemical study. Brain Res. 846 (1), 129-136.
- Nica, I., Deprez, M., Nuttin, B., Aerts, J.M., 2017. Automated assessment of endpoint and kinematic features of skilled reaching in rats. Front Behav. Neurosci. 11, 255.
- Nikkhah, Rosenthal, C., Falkenstein, G., Roedter, A., Papazoglou, A., Brandis, A., 2009. Microtransplantation of dopaminergic cell suspensions: further characterization and optimization of grafting parameters. Cell Transpl. 18, 119–133.
- Nikkhah, G., Rosenthal, C., Hedrich, H.J., Samii, M., 1998. Differences in acquisition and full performance in skilled forelimb use as measured by the 'staircase test' in five rat strains. Behav. Brain Res 92, 85-95.
- Oliveras-Salvá, M., Van de Perren, A., Casadei, N., Stroobants, S., Nuber, S., D'Hooge, R., Van den Haute, C., Baekelandt, V., 2013. rAAV2/7 vector-mediated overexpression of alpha-synuclein in mouse substantia nigra induces protein aggregation and progressive dose-dependent neurodegeneration. Mol. Neurodegener. 8, 44.
- Olsson, M., Nikkhah, G., Bentlage, C., Björklund, 1995. Forelimb akinesia in the rat Parkinson model: differential effects of dopamine agonists and nigral transplants as assessed by a new stepping test. J. Neurosci. 15, 3863-3875.
- Østergaard, F.G., Himmelberg, M.M., Laursen, B., Siebner, H.R., Wade, A.R., Christensen, K.V., 2020. Classification of α -synuclein-induced changes in the AAV α-synuclein rat model of Parkinson's disease using electrophysiological measurements of visual processing. Sci. Rep. 10 (1), 11869. https://doi.org/ 10.1038/s41598-020-68808-3. Published 2020 Jul 17.
- Palfreyman, J.W., Thomas, D.G., Ratcliffe, J.G., Graham, D.I., 1979. Glial fibrillary acidic protein (GFAP): purification from human fibrillary astrocytoma, development and validation of a radioimmunoassay for GFAP-like immunoactivity. J. Neurol. Sci. 41, 101-113
- Paolicelli, R.C., Sierra, A., Stevens, B., Tremblay, M.E., Aguzzi, A., Ajami, B., Amit, I., Audinat, E., Bechmann, I., Bennett, M., Bennett, F., Bessis, A., Biber, K., Bilbo, S., Blurton-Jones, M., Boddeke, E., Brites, D., Brône, B., Brown, G.C., Butovsky, O., Carson, M.J., Castellano, B., Colonna, M., Cowley, S.A., Cunningham, C.,

- Davalos, D., De Jager, P.L., de Strooper, B., Denes, A., Eggen, B.J.L., Eyo, U., Galea, E., Garel, S., Ginhoux, F., Glass, C.K., Gokce, O., Gomez-Nicola, D., González, B., Gordon, S., Graeber, M.B., Greenhalgh, A.D., Gressens, P., Greter, M., Gutmann, D.H., Haass, C., Heneka, M.T., Heppner, F.L., Hong, S., Hume, D.A., Jung, S., Kettenmann, H., Kipnis, J., Koyama, R., Lemke, G., Lynch, M., Majewska, A., Malcangio, M., Malm, T., Mancuso, R., Masuda, T., Matteoli, M., McColl, B.W., Miron, V.E., Molofsky, A.V., Monje, M., Mracsko, E., Nadjar, A., Neher, J.J., Neniskyte, U., Neumann, H., Noda, M., Peng, B., Peri, F., Perry, V.H., Popovich, P.G., Pridans, C., Priller, J., Prinz, M., Ragozzino, D., Ransohoff, R.M., Salter, M.W., Schaefer, A., Schafer, D.P., Schwartz, M., Simons, M., Smith, C.J., Streit, W.J., Tay, T.L., Tsai, L.H., Verkhratsky, A., von Bernhardi, R., Wake, H., Wittamer, V., Wolf, S.A., Wu, L.J., Wyss-Coray, T., 2022. Microglia states and nomenclature: a field at its crossroads. Neuron 110, 3458-3483.
- Paxinos, G., Watson, C., 2013. The Rat Brain in Stereotaxic Coordinates, 7th edition. Elsevier Academic Press, pp. 1-480.
- Pençe, S., 2002. Paw preference in rats. J. Basic Clin. Physiol. Pharm. 13, 41-49. Perez, R.G., Waymire, J.C., Lin, E., Liu, J.J., Guo, F., Zigmond, M.J., 2002. A role for alpha-synuclein in the regulation of dopamine biosynthesis. J. Neurosci. 22,
- Polymeropoulos, M.H., Lavedan, C., Leroy, E., Ide, S.E., Dehejia, A., Dutra, A., Pike, B., Root, H., Rubenstein, J., Boyer, R., Stenroos, E.S., Chandrasekharappa, S., Athanassiadou, A., Papapetropoulos, T., Johnson, W.G., Lazzarini, A.M., Duvoisin, R. C., Di Iorio, G., Golbe, L.I., Nussbaum, R.L., 1997. Mutation in the alpha-synuclein gene identified in families with Parkinson's disease. Science 276, 2045–2047.
- Poulin, J.F., Zou, J., Drouin-Ouellet, J., Kim, K.Y.A., Cicchetti, F., Awatramani, R.B., 2014. Defining midbrain dopaminergic neuron diversity by single-cell gene expression profiling. Cell Rep. 9, 930-943.
- Rajput, A.H., 1992. Frequency and cause of Parkinson's disease. Can. J. Neurol. Sci. 19, 103-107
- Ratzka, A., Kalve, I., Özer, M., Nobre, A., Wesemann, M., Jungnickel, J., Köster-Patzlaff, C., Baron, O., Grothe, C., 2012. The colayer method as an efficient way to genetically modify mesencephalic progenitor cells transplanted into 6-OHDA rat model of Parkinson's disease. Cell Transpl. 21, 749-762.
- Reyes, S., Fu, Y., Double, K., Thompson, L., Kirik, D., Paxinos, G., Halliday, G.M., 2012. GIRK2 expression in dopamine neurons of the substantia nigra and ventral tegmental area. J. Comp. Neurol. 520, 2591–2607.
- Rumpel, R., Hohmann, M., Klein, A., Wesemann, M., Baumgärtner, W., Ratzka, A., Grothe, C., 2015. Transplantation of fetal ventral mesencephalic progenitor cells overexpressing high molecular weight fibroblast growth factor 2 isoforms in 6hydroxydopamine lesioned rats. Neuroscience 286, 293-307.
- Schallert, T., Fleming, S.M., Leasure, J.L., Tillerson, J.L., Bland, S.T., 2000. CNS plasticity and assessment of forelimb sensorimotor outcome in unilateral rat models of stroke, cortical ablation, parkinsonism and spinal cord injury. Neuropharmacology 39, 777–787.
- Schwab, R.S., 1960. Progression and prognosis in Parkinson's disease. J. Nerv. Ment. Dis. 130, 556-566.
- Sherer, T.B., Betarbet, R., Kim, J.H., Greenamyre, J.T., 2003, Selective microglial activation in the rat rotenone model of Parkinson's disease. Neurosci, Lett. 341,
- Simons, E., Fleming, S.M., 2023. Role of rodent models in advancing precision medicine for Parkinson's disease. Handb. Clin. Neurol. 193, 3-16.
- Soundy, A., Stubbs, B., Roskell, C., 2014. The experience of Parkinson's disease: a systematic review and meta-ethnography. ScientificWorldJournal 2014, 613592. Spillantini, M.G., Schmidt, M.L., Lee, V.M., Trojanowski, J.Q., Jakes, R., Goedert, M.,
- 1997. Alpha-synuclein in Lewy bodies. Nature 388, 839-840.
- Stößel, M., Rehra, L., Hasstert-Talini, K., 2017. Reflex-based grasping, skilled forelimb reaching, and electrodiagnostic evaluation for comprehensive analysis of functional recovery-The 7-mm rat median nerve gap repair model revisited. Brain Behav. 7, e00813.
- Su, D., Cui, Y., He, C., Yin, P., Bai, R., Zhu, J., Lam, J., Zhang, J., Yan, R., Zheng, X., Wu, J., Zhao, D., Wang, A., Zhou, M., Feng, T., 2025. Projections for prevalence of Parkinson's disease and its driving factors in 195 countries and territories to 2050: modelling study of Global Burden of Disease Study 2021. BMJ 388, e080952. Published 2025 Mar 5.
- Su, X., Federoff, H.J., Maguire-Zeiss, K.A., 2009. Mutant alpha-synuclein overexpression mediates early proinflammatory activity. Neurotox. Res 16, 238-254.
- Sun, H., Liang, R., Yang, B., Zhou, Y., Liu, M., Fang, F., Ding, J., Fan, Y., Hu, G., 2016. Aquaporin-4 mediates communication between astrocyte and microglia: implications of neuroinflammation in experimental Parkinson's disease. Neuroscience 317, 65-75.
- Takamatsu, Y., Fujita, M., Ho, G.J., Wada, R., Sugama, S., Takenouchi, T., Waragai, M., Masliah, E., Hashimoto, M., 2018. Motor and nonmotor symptoms of Parkinson's disease: antagonistic pleiotropy phenomena derived from α -synuclein evolvability? Park, Dis. 2018, 5789424.
- Thompson, L., Barraud, P., Andersson, E., Kirik, D., Björklund, A., 2005. Identification of dopaminergic neurons of nigral and ventral tegmental area subtypes in grafts of fetal ventral mesencephalon based on cell morphology, protein expression, and efferent projections. J. Neurosci. 25, 6467-6477.
- Timmer, M., Grosskreuz, J., Schlesinger, F., Krampfl, K., Wesemann, M., Just, L. Bufler, J., Grothe, C., 2006. Dopaminergic properties and function after grafting of attached neural precursor cultures. Neurobiol. Dis. 21, 587-606.
- Tolosa, E., Martí, M.J., Valldeoriola, F., Molinuevo, J.L., 1998. History of levodopa and dopamine agonists in Parkinson's disease treatment. Neurology 50, S2-S10 discussion S44-8.

- Tong, J., Ang, L.C., Williams, B., Furukawa, Y., Fitzmaurice, P., Guttman, M., Boileau, I., Hornykiewicz, O., Kish, S.J., 2015. Low levels of astroglial markers in Parkinson's disease: relationship to α-synuclein accumulation. Neurobiol. Dis. 82, 243–253.
- Tumas, V., Aureliano, M.J., Rieder, C.R.M., Schuh, A., Ferraz, H.B., Borges, V., Soares, M. C., Boone, D.L., Silva, C., Costa, M.C., Silva, D., Carmo, A., Mikael, L.R., Santos-Lobato, B.L., Rosso, A., Vilaça, C.O., Braga-Neto, P., Gomes, A., Carvalho, C., Letro, G.H., Nicaretta, D.H., Coletta, M., Barbosa, E.R., Cury, R.G., Cardoso, F., Camargos, S.T., Mata, I.F., 2025. Modifiable risk factors associated with the risk of developing Parkinson's disease: a critical review. Arq. Neuropsiquiatr. 83 (3), 1–10.
- Tysnes, O.B., Storstein, A., 2017. Epidemiology of Parkinson's disease. J. Neural Transm. (Vienna) 124 (8), 901–905.
- Unis, A.S., Petracca, F., Diaz, J., 1991. Somatic and behavioral ontogeny in three rat strains: preliminary observations of dopamine-mediated behaviors and brain D-1 receptors. Prog. Neuropsychopharmacol. Biol. Psychiatry 15, 129–138.
- Van der Perren, A., Toelen, J., Carlon, M., Van den Haute, C., Coun, F., Heeman, B., Reumers, V., Vandenberghe, L.H., Wilson, J.M., Debyser, Z., Baekelandt, V., 2011. Efficient and stable transduction of dopaminergic neurons in rat substantia nigra by rAAV 2/1, 2/2, 2/5, 2/6.2, 2/7, 2/8 and 2/9. Gene Ther. 18, 517–527.
- Vercueil, L., Benazzouz, A., Deransart, C., Bressand, K., Marescaux, C., Depaulis, A., Benabid, A.L., 1998. High-frequency stimulation of the subthalamic nucleus suppresses absence seizures in the rat: comparison with neurotoxic lesions. Epilepsy Res 31, 39–46.
- Volpicelli-Daley, L.A., Luk, K.C., Patel, T.P., Tanik, S.A., Riddle, D.M., Stieber, A., Meaney, D.F., Trojanowski, J.Q., Lee, V.M.Y., 2011. Exogenous α-synuclein fibrils induce Lewy body pathology leading to synaptic dysfunction and neuron death. Neuron 72, 57–71.

- von Hövel, F.F., Rumpel, R., Ratzka, A., Schneider, D., Grothe, C., 2019. AAV2/DJ-mediated alpha-synuclein overexpression in the rat substantia nigra as early stage model of Parkinson's disease. Cell Tissue Res 378, 1–14.
- Wakabayashi, K., Takahashi, H., 1997. Neuropathology of autonomic nervous system in Parkinson's disease. Eur. Neurol. 38 (2), 2–7.
- Whishaw, I.Q., Whishaw, P., Gorny, B., 2008. The structure of skilled forelimb reaching in the rat: a movement rating scale. J. Vis. Exp. 8 816.
- Whishaw, I.Q., Woodward, N.C., Miklyaeva, E., Pellis, S.M., 1997. Analysis of limb use by control rats and unilateral DA-depleted rats in the Montoya staircase test: movements, impairments and compensatory strategies. Behav. Brain Res 89, 167-177.
- Winner, B., Jappelli, R., Maji, S.K., Desplats, P.A., Boyer, L., Aigner, S., Hetzer, C., Loher, T., Vilar, M., Campioni, S., Tzitzilonis, C., Soragni, A., Jessberger, S., Mira, H., Consiglio, A., Pham, E., Masliah, E., Gage, F.H., Riek, R., 2011. In vivo demonstration that alpha-synuclein oligomers are toxic. Proc. Natl. Acad. Sci. USA 108, 4194–4199.
- Wong, Y.C., Krainc, D., 2017. α -synuclein toxicity in neurodegeneration: mechanism and therapeutic strategies. Nat. Med 23, 1–13.
- Ye, H., Robak, L.A., Yu, M., Cykowski, M., Shulman, J.M., 2023. Genetics and pathogenesis of Parkinson's syndrome. Annu Rev. Pathol. 18, 95–121.
- Zhang, W., Wang, T., Pei, Z., Miller, D.S., Wu, X., Block, M.L., Wilson, B., Zhang, W., Zhou, Y., Hong, J.S., Zhang, J., 2005. Aggregated alpha-synuclein activates microglia: a process leading to disease progression in Parkinson's disease. Faseb J. 19, 533–542.
- Zheng, T., Zhang, Z., 2021. Activated microglia facilitate the transmission of α -synuclein in Parkinson's disease. Neurochem. Int. 148, 105094.